

# Progress on Electrospun Composite Fibers Incorporating Bioactive Glass: An Overview

Farnaz Ghorbani, Theresa Reiter, Liliana Liverani, Dirk W. Schubert, Aldo R. Boccaccini,\* and Judith A. Roether\*

Electrospinning is a promising approach for the development of fibrous tissue engineering (TE) scaffolds suitable for hard and soft tissues. Apart from physico-mechanical properties, electrospun fibers are required to incorporate bioactive cues to control cellular functions, including facilitating biomineralization and osteogenic differentiation in case of bone TE, as well as vascularization, to support successful tissue regeneration. In recent years, bioactive glass (BG) addition to electrospun biopolymer fibers has shown promising results in enhancing the properties of fibers, including the improvement of biological performance. In this article, a comprehensive overview of BG-containing electrospun polymer composite fibers is presented, identifying the parameters that affect the mechanical properties as well as the biological response in vivo and in vitro. Subsequently, the effects of BG addition on the properties of the scaffolds are discussed. Recent developments in the fields of bone regeneration, wound healing, and drug delivery using BG-containing electrospun fibrous scaffolds are described in detail. Essential aspects related to BG-polymer composite fibers for translational research in TE are highlighted for future research in this field.

## 1. Introduction

Among various technologies for fabrication of scaffolds for tissue engineering (TE), electrospinning has gained increasing attention

over the years because of its simplicity, cost-effectiveness, and its ability to produce fibrous scaffolds with relatively high porosities and large surface-area-to-volume ratios. Electrospun scaffolds can mimic the native extracellular matrix (ECM) of tissues enabling cell attachment and infiltration and making tissue remodeling possible.<sup>[1]</sup> Electrospun fibers can provide adequate mechanical properties and promote cell adhesion, proliferation, differentiation, and internal vascularization.<sup>[2–4]</sup> Herein, well-controlled electrospun polymer fibers that are tailored by considering various intrinsic and extrinsic processing parameters as well as solution parameters, such as polymer solution concentration, pressure, humidity, viscosity, surface tension, voltage, injection rate, and collector characteristics, can influence the microstructure and orientation of fibers and, as a result, the effectiveness of


the scaffolds for new tissue ingrowth.<sup>[5,6]</sup> In this regard, unidirectionally oriented fibers are effective in supporting directional cell growth, orientation, and aligned regeneration of damaged tissue.<sup>[7,8]</sup>

The chemical composition of the fibers is another influential factor dictating the success of their application in TE. Over the past decades, numerous natural and synthetic polymers, such as collagen, alginate, poly(lactic acid-co-glycolic acid) (PLGA), and poly( $\epsilon$ -caprolactone) (PCL), have been investigated to produce nanofibrous scaffolds<sup>[9–13]</sup> due to biocompatibility, degradability, ease of processing, and the ability to produce nanostructures resembling features of natural tissues. However, hydrophobicity and poor bioactivity of (synthetic) polymeric constructs and inadequate mechanical properties of single-component polymeric scaffolds have motivated the development of multicomponent or functionalized fibers using active biological cues.<sup>[14,15]</sup> Combining the advantages of different materials with complementary properties leads to multiphase materials, composites, or hybrids with superior physicochemical and biological properties providing versatile possibilities for TE applications. Significantly, electrospinning using polymers, bioactive, and bioresorbable inorganic materials has been investigated intensively to fabricate composite fibers for bone and soft tissue regeneration.<sup>[16–18]</sup> Over the past two decades, bioactive glasses (BGs), i.e., surface-reactive inorganic materials with an amorphous structure, have been widely used for fabricating composite fibers because of the functionalities they can impart to polymeric-based composites, including bioactivity,

F. Ghorbani, T. Reiter, L. Liverani, A. R. Boccaccini  
Institute of Biomaterials, Department of Materials Science and Engineering  
University of Erlangen-Nuremberg  
Cauerstrasse 6, 91058 Erlangen, Germany  
E-mail: aldo.boccaccini@fau.de

D. W. Schubert, J. A. Roether  
Institute of Polymeric Materials  
Department of Materials Science and Engineering  
University of Erlangen-Nuremberg  
Martensstrasse 7, 91058 Erlangen, Germany  
E-mail: judith.roether@fau.de

D. W. Schubert, A. R. Boccaccini  
Bavarian Polymer Institute  
KeyLab Advanced Fiber Technology  
Dr. Mack-Strasse 77, 90762 Fürth, Germany

 The ORCID identification number(s) for the author(s) of this article can be found under <https://doi.org/10.1002/adem.202201103>.

© 2022 The Authors. Advanced Engineering Materials published by Wiley-VCH GmbH. This is an open access article under the terms of the Creative Commons Attribution License, which permits use, distribution and reproduction in any medium, provided the original work is properly cited.

DOI: 10.1002/adem.202201103

osteoconductivity, osteogenic performance, acceleration of vascularization, biodegradability, and drug delivery functionality.<sup>[19–23]</sup>

This review aims to present a comprehensive overview of composite micro/nanofibers incorporated with BG particles, which have been developed by electrospinning in the past decades (Figure 1). The review focuses on the processing–structure–property relationships of BG-containing fibers. Therefore, we extensively review chemical compositions, microstructures, and properties of BG-incorporated electrospun composite fibers to present a complete assessment of the state of the art with focus on bioactive scaffold fabrication for bone and soft tissue regeneration. The Web of Science database was used employing the keywords: “electrospinning” and “bioactive glasses”, “composites” or “fibers”. In addition, the search was carried out for the years

2002–2022. Only papers that reported an application in bone or soft tissue regeneration were considered. Here, we concentrate on current advances and offer perspectives on the challenges and opportunities for future translational development. The review thus aimed to be balanced and to reflect the current state of the art based on contributions by different groups around the world.

## 2. Bioactive Glass-Containing Composite Fibers

### 2.1. The Effect of Bioactive Glass Addition on Electrospun Fiber Fabrication: Comparison with Other Inorganic Fillers

In recent decades, various inorganic components have been considered to reinforce electrospun polymer composite fibers.

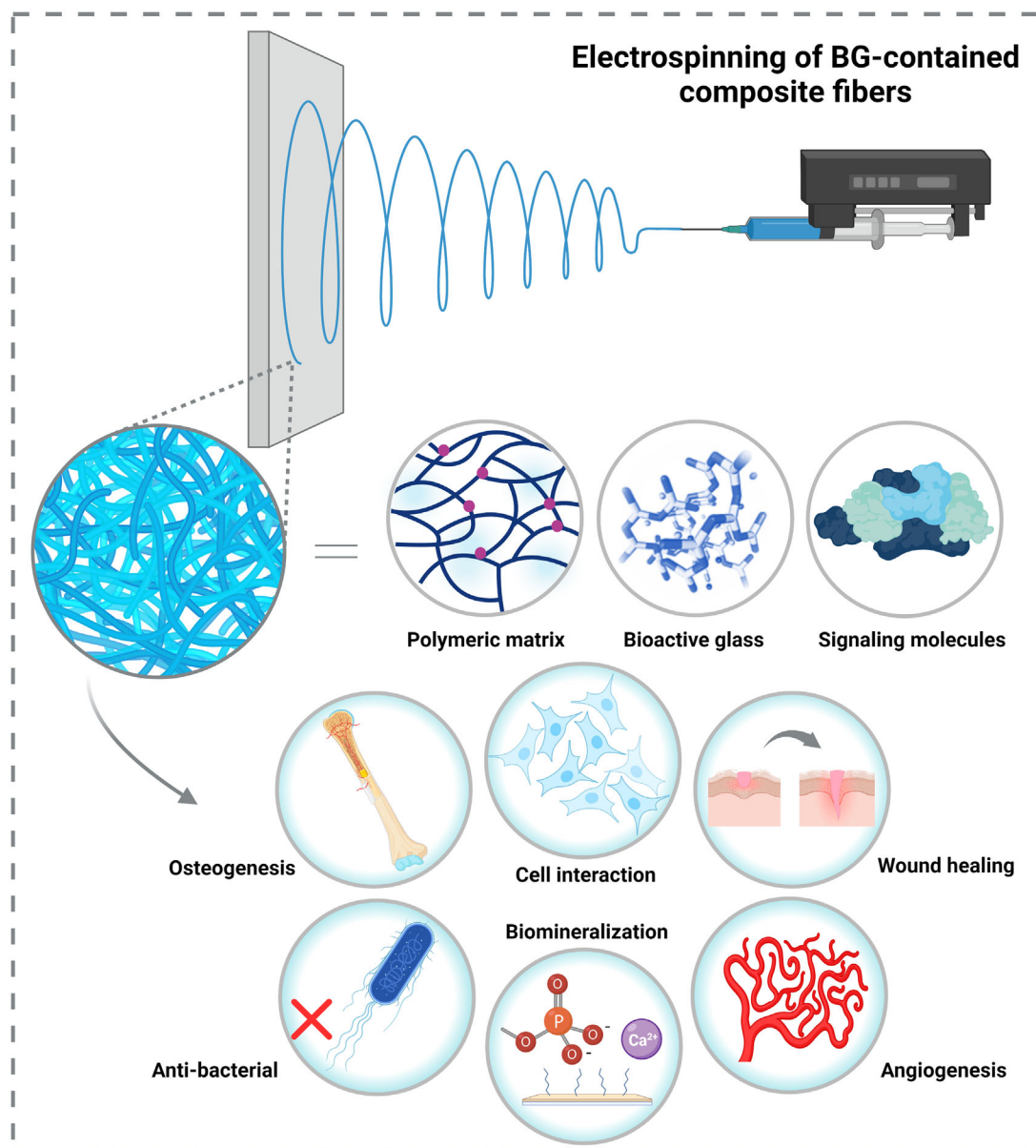


**Figure 1.** Schematic illustration of the fabrication of electrospun BG-containing composite fibers and major properties and functionalities achieved, including biom mineralization, osteogenesis, angiogenesis, and antibacterial activity. Created with BioRender.com.

The incorporation of bioactive and bioresorbable inorganic materials into polymers has been widely investigated for biomedical applications.<sup>[24]</sup> Inorganic components are introduced using either direct or indirect strategies, such as electrospinning of composite solution/suspensions,<sup>[25]</sup> or by layer-by-layer stacking of electrospun fiber mats.<sup>[26]</sup> Bioactivity (mineralization ability) is recognized as a critical requirement for bone TE; hence, calcium phosphates like hydroxyapatite (HA) as well as BGs, which can support the in situ formation of hydroxyl carbonate apatite,<sup>[27]</sup> have found versatile applications in the fabrication of TE scaffolds. HA and BGs are attractive bioactive inorganic materials due to the fact that they exhibit potential to improve bone regeneration,<sup>[28,29]</sup> through the activation of osteogenic genes<sup>[30]</sup> and angiogenesis.<sup>[31,32]</sup> Applications of BG-containing electrospun fibers in soft TE and wound healing are also emerging.<sup>[19,33,34]</sup> In this regard, Shalumon et al.<sup>[35]</sup> compared electrospun composite nanofibers composed of nano

HA-PCL-chitosan and BG nanoparticles (45S5 BG composition, size: 20–80 nm)-PCL-chitosan with the similar concentration (3 wt%) of inorganic components. The results showed that both types of inorganic particles increased the alkaline phosphatase (ALP) activity of human periodontal ligament fibroblast cells (hPDLFs), while embedding BG nanoparticles demonstrated significant improvement in hPDLFs and osteoblast-like cell (MG-63 cell line) adhesion and proliferation (Figure 2A1-A10). BG (composition: silicate-based 45S5 and borate-based 13-93B3) and HA with a concentration of 10 wt% were incorporated into PCL nanofibrous scaffolds. According to observations, composite fibers showed bioactive behavior throughout a period of 30 days immersion in SBF solution. Here, the deposition rate of calcium phosphate layer precipitation was higher in HA-containing constructs compared to BG-containing ones. Moreover, the mineralization potential of 13-93B3 BG-containing fibers was higher compared to that of 45S5 BG-containing ones.<sup>[36]</sup> In a parallel

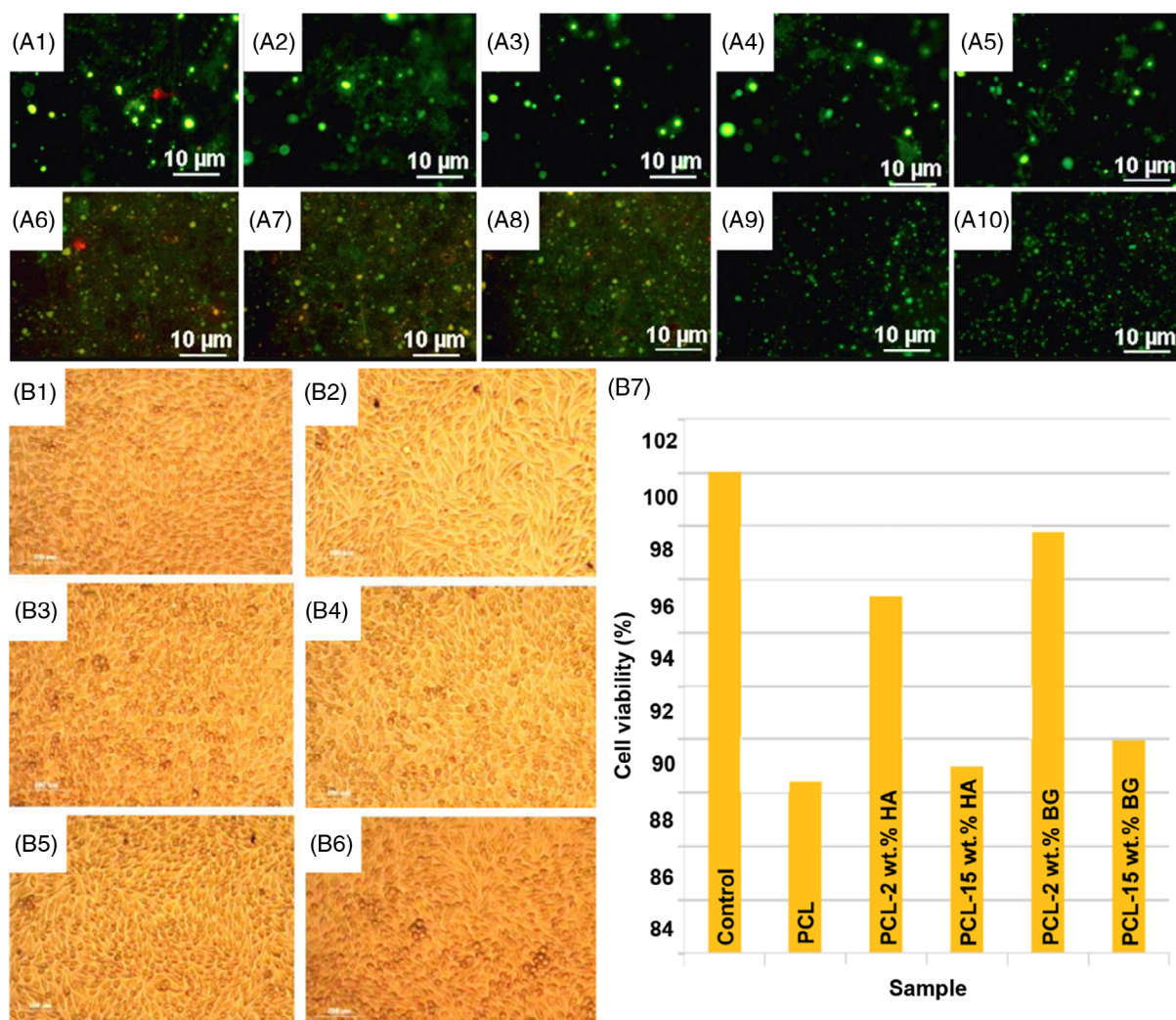


**Figure 2.** A1-A10 Live-dead cell staining after (A1-A5) 12 h and (A6-A10) 48 h of culturing hPDLF cells on the (A1,A6) control group, PCL fibers contained (A2,A7) 1.5 wt% HA, (A3,A8) 3 wt% HA, (A4,A9) 1.5 wt% BG, and (A5,A10) 3 wt% BG. Reproduced with permission.<sup>[35]</sup> Copyright 2013, American Scientific Publishers. (B1-B7) Cell viability after 24 h of culturing the L-929 mouse fibroblasts using MTT assay. Optical microscopic image of cell culture on B1) control group, B2) PCL, B3) PCL-2 wt% HA, B4) PCL-15 wt% HA, B5) PCL-2 wt% BG, B6) PCL-15 wt% BG, and B7) quantitative cell viability comparison. Reproduced with permission<sup>[40]</sup> under the open access Creative Common CC BY license.

investigation by Ródenas-Rochina et al.,<sup>[37]</sup> the potential of HA (size: 200 nm) or BG (composition: 45S5, size: 20  $\mu\text{m}$ , concentration: up to 20% (wt%))-containing PCL scaffolds for bone regeneration was evaluated. Both scaffolds indicated adequate mechanical strength as well as a suitable porous structure for cellular colonization. Composite constructs support the behavior of MC3T3-E1 cells (an osteoblast precursor cell line from mouse calvaria); however, for BG-PCL scaffolds, the filler concentration was considered a crucial parameter: scaffolds with 5% filler increased the cell adhesion without any positive effect on cell differentiation. Improved cell adhesion originated from increased protein adsorption as a function of BG addition. In contrast, HA addition inhibited cell differentiation up to 28 days. Besides, BG-containing polylactic acid (PLA) scaffolds were compared with  $\beta$ -tricalcium phosphate ( $\beta$ -TCP) incorporated PLA. Results revealed that the relative ALP/DNA ratio of human adipose stem cells (ASCs) was higher when BG was added to the constructs in comparison with those containing  $\beta$ -TCP even though lower overall cell numbers were observed in BG-PLA composite scaffolds.<sup>[38]</sup> Similarly, Goh et al.<sup>[39]</sup> confirmed the effectiveness of BG (CeBG/CuBG/AgBG, size: 79–84 nm)-containing fibers compared to those with HA or  $\beta$ -TCP in terms of the acceleration of bone formation. A similar phenomenon was also observed by Sunandhakumari et al.<sup>[40]</sup> These studies indicate better performance of BG nanoparticles (composition: 34% SiO<sub>2</sub>, 4.6% MgO, 44.7% CaO, 16.2% P<sub>2</sub>O<sub>5</sub>, and 0.5% CaF<sub>2</sub> (wt%)) in enhancing cell viability, attachment, proliferation, and differentiation of L-929 mouse fibroblast cells compared with nano HA particles (Figure 2B1-B7).

## 2.2. Effect of Bioactive Glass Addition on Electrospun Fiber Diameter

Incorporation of BG particles in the electrospun solution leads to specific effects regarding morphology and diameter of the fibers (Table 1). In this regard, Moura et al.<sup>[41]</sup> reported the influence of BG (composition: SiO<sub>2</sub>:CaO:P<sub>2</sub>O<sub>5</sub>:CoO:Ag<sub>2</sub>O (mol%) = 50:40:5:2.5:2.5) addition on the diameter of PCL fibers (Figure 3A1-A5), using a less toxic solvent like acetone. It was observed that increasing BG particle (size: 32  $\pm$  17 nm) content from 0.25 to 0.75 wt% led to an increase in fiber diameter, which was attributed to the higher viscosity of the suspension. A parallel investigation determined that incorporating BG (composition: 45S5, concentration: 20 wt%, size: <20  $\mu\text{m}$ ) in chitosan-polyethylene oxide solution, prepared using a benign solvent (aqueous acetic acid), resulted in a slight increase in fiber diameter. Here, doping BG with Zn led to a reduction in fiber diameter. However, all BG-containing fibers indicated higher Young's modulus compared with BG-free fibers.<sup>[42]</sup> A similar influence of BG on fiber morphology was observed in research reported by Schuhladden et al.<sup>[43]</sup> Here, the addition of BG particles (composition: 5.5% Na<sub>2</sub>O-11.1% K<sub>2</sub>O-4.6% MgO-18.5% CaO-56.6% B<sub>2</sub>O<sub>3</sub>-3.7% P<sub>2</sub>O<sub>5</sub> (wt%), size: 5–20  $\mu\text{m}$ ) to PCL-methylcellulose electrospun fibers increased the fiber diameter and enhanced bioactivity potential. In a similar investigation, Liverani et al.<sup>[44]</sup> analyzed BG particles (composition: 45S5, size: 2  $\mu\text{m}$  and 20–80 nm) as an addition to PCL-chitosan solutions made using benign solvents (in particular acetic acid and formic

acid) and investigated microstructure, mechanical properties, and bioactivity of the produced fibers. Regarding the average fiber diameter, a slight increase in fiber diameter was detected after adding both sizes of BG particles. Besides, nano-sized BG particles provided a narrower size distribution of fibers compared to micron-sized fibers. In this investigation, BG-containing fibers exhibited a reduction in mechanical strength in comparison to BG-free fibers due to inhomogeneity in the fiber diameter (e.g., fibers with irregular shape and with diameter varying along the fiber) and possible weak BG-polymer interfacial adhesion. Here, BG-embedded fibers indicated the precipitation of HA after 1 day soaking in the SBF solution, which proved the bioactivity of the composite fibers. Similarly, composite fibers based on BG (composition: SiO<sub>2</sub> 55%-CaO 35%-P<sub>2</sub>O<sub>5</sub> 6.5%-Ag<sub>2</sub>O 3.5% (wt%), concentration: 5 and 10 wt%) particles incorporated in polyvinyl alcohol (PVA)-sodium alginate indicated fiber diameters three times higher than those of pure polymeric fibers.<sup>[45]</sup> Electrospun chitosan-polyethylene oxide nanofibers were incorporated with BG particles (composition: 45S5, concentration: 15 wt%, size: 10–20  $\mu\text{m}$ ) in the investigation of Boschetto et al.<sup>[46]</sup> for coating the surface of titanium-based orthopedic implants. Here, ultrathin fibers were produced that originate from phase separation of charged droplets generated during electrospinning under electrostatic and drag forces, as well as gravity. However, the incorporation of BG led to 1.6 times increase in the average fiber diameter. In contrast, Serio et al.<sup>[47]</sup> indicated a reduction in diameter of poly L-lactic acid (PLLA) fibers, which were incorporated with BG particles (composition: 48% SiO<sub>2</sub>-18% Na<sub>2</sub>O-30% CaO-3% P<sub>2</sub>O<sub>5</sub>-0.43% B<sub>2</sub>O<sub>3</sub>-0.57% Al<sub>2</sub>O<sub>3</sub> (mol%), size: 2  $\mu\text{m}$ , concentration: 7%(w/v)) for bone and soft tissue applications. This finding was attributed to the influence of the BG particles on the rheology and conductivity of the composite solution. However, the addition of BG significantly increased the elastic modulus in comparison to that of BG-free fibers. Moreover, embedding BG particles in fibers improved the formation of HA-like layers after immersion in SBF solution for 21 days (Figure 3B1-B8). On the other hand, poly(glycerol-sebacate)-PCL composite fibers were incorporated with BG (composition: 13-93 and 13-93BS, size: 5–20  $\mu\text{m}$ , concentration: 30 wt%) in an investigation by Luginina and co-workers,<sup>[48]</sup> employing a green solvent, i.e., acetic acid. BG addition showed no significant differences in the average fiber diameter.

## 2.3. Effect of Bioactive Glass Concentration on Electrospun Fiber Characteristics

In composite fibers, a maximum volume fraction of particles can be incorporated into the polymer matrix without a negative influence on processability. Accordingly, to ensure bioactive potential and the formation of a mineralized layer on the fiber surfaces, a minimum amount above a certain threshold of the inorganic component needs to be added (Table 1). In this regard, the addition of 0.25 wt% BG nanoparticles (composition: SiO<sub>2</sub>:CaO:P<sub>2</sub>O<sub>5</sub>:CoO:Ag<sub>2</sub>O (mol%) = 50:40:5:2.5:2.5, size: 32  $\pm$  17 nm) to the PCL matrix showed no evidence of HA formation, while samples containing 0.5 and 0.75 wt% BG nanoparticles showed cauliflower-like HA structures after 21 days of immersion in SBF solution. These findings indicated that 0.25 wt% was



**Table 1.** Influence of BG addition and its concentration on composite fibers properties.

Composition	BG features	Solvent	Doping ion	Application	Properties	References
PCL-BG	Composition: SiO <sub>2</sub> :CaO:P <sub>2</sub> O <sub>5</sub> : CoO:Ag <sub>2</sub> O (mol%) = 50:40:5:2.5:2.5 Size: 32 ± 17 nm Concentration: 0.25–0.75 wt%	Acetone	Cobalt and silver	Wound healing	-Increasing fiber diameter as a function of BG enhancement -Accelerating weight loss rate  -Higher ultimate tensile strength as a function BG enhancement -Enhancing angiogenic performance -Inducing anti-bacterial features	[41]
Chitosan-polyethylene oxide-BG	Composition: 45S5 Size: <20 μm Concentration: 20 wt%	Aqueous acetic acid	Zinc	Wound healing	-Slight increase in fiber diameter -Reduction in fiber diameter as a function of Zn -Increasing Young's modulus	[42]
PCL-methylcellulose-BG	Composition: 5.5% Na <sub>2</sub> O-11.1% K <sub>2</sub> O-4.6% MgO-18.5% CaO-56.6% B <sub>2</sub> O <sub>3</sub> -3.7% P <sub>2</sub> O <sub>5</sub> (wt%) Size: 5–20 μm	Acetic acid	–	Wound dressing	-Increasing fiber diameter as a function of BG addition  -Bioactivity enhancement	[43]
Poly(glycerol-sebacate)-PCL-BG	Composition: 13-93 and 13-93BS Size: 5–20 μm Concentration: 30 wt%	Acetic acid	–	Soft TE	-Increasing fiber diameter as a function of BG addition, but there were no significant differences in average fiber diameter	[48]
PCL-chitosan-BG	Composition: 45S5 Size: 2 μm and 20–80 nm Concentration: 30 wt%	Acetic acid–formic acid	–	Bone TE	-HA precipitation -Increasing in fiber diameter as a function of BG addition -Reduction in mechanical strength	[44]
PVA-sodium alginate-BG	Composition: SiO <sub>2</sub> 55%-CaO 35%-P <sub>2</sub> O <sub>5</sub> 6.5%-Ag <sub>2</sub> O 3.5% (wt%) Concentration: 5 and 10% (w/w)	DI water	–	Wound healing	-Increasing fiber diameter -Bioactivity -Improvement in elastic modulus -Reduction in compressive strength	[45]
Chitosan-poly ethylene oxide-BG	Composition: Standard 45S5 Size: 10–20 μm Concentration: 15 wt%	Acetic acid–water	–	Orthopedic Applications	-1.6 times increase in average fiber diameter	[46]
PLLA-BG	Composition: 48% SiO <sub>2</sub> -18% Na <sub>2</sub> O-30% CaO-3% P <sub>2</sub> O <sub>5</sub> -0.43% B <sub>2</sub> O <sub>3</sub> -0.57% Al <sub>2</sub> O <sub>3</sub> (mol%) Size: 2 μm Concentration: 7%w/v	Dichloromethane-acetone	–	Bone and soft TE	-Reduction in fiber diameter as a function of BG addition -BG addition increased elastic modulus -Improvement in the formation of HA-like layers after immersion in the SBF solution for 21 days after embedding the BG in fibers	[47]
POC-BG	Composition: 70SiO <sub>2</sub> -25CaO-5P <sub>2</sub> O <sub>5</sub> Concentration: 5, 10, and 15% w/w	Ethanol	–	Bone TE	-Increasing glass transition temperature -increasing modulus and strength -Decreasing elongation at break	[49]
Chitosan-PVA- BG nanoparticles	Composition: 76% SiO <sub>2</sub> -18% CaO-6% P <sub>2</sub> O <sub>5</sub> (wt%)  Size: 800 nm Concentration: 5, 10, 20, and 40 wt%	Trifluoroacetic acid-dichloromethane	–	Wound healing	-Low concentration of BG nanoparticles enhanced yield strength and breaking strength but reduced elongation percentage -Higher concentration of BG nanoparticles decreased tensile strength and elongation percentage -Biocompatibility	[50]

**Table 1.** Continued.

Composition	BG features	Solvent	Doping ion	Application	Properties	References
PCL-BG	Composition: 13-93 Size: <106 $\mu\text{m}$ Concentration: 1, 5, and 10 wt%	Acetone	–	Bone TE	-Anti-inflammatory behaviour -Angiogenesis -Increasing fiber diameter as a function of BG addition	[51]
PCL-TES-BG	Composition: 45S5 Size: 2 $\mu\text{m}$ Concentration: 30 wt%	Acetic acid	–	Biomedical applications	-Plate-like HA formation in SBF solution (30 days immersion) -Reduction in fiber diameter by BG particles addition -BG particles support in vitro bioactivity and mineralization of hydroxyapatite layers after 7 days of immersion in the SBF solution -BG particles does not negatively affect or inhibit the viability of ST-2 cell cells	[52]

insufficient to induce mineralization, which was attributed to the encapsulation of particles within the polymeric fiber. The obtained results furthermore indicated a faster weight loss and higher ultimate tensile strength as a function of BG content.<sup>[41]</sup> Composite fibers composed of PVA, sodium alginate, and BG (composition:  $\text{SiO}_2$  55%-CaO 35%- $\text{P}_2\text{O}_5$  6.5%- $\text{Ag}_2\text{O}$  3.5% (wt%), concentration: 5 and 10 wt%) showed that a higher BG content resulted in a faster degradation.<sup>[45]</sup> The observation of cauliflower-like HA on the surface of BG-containing scaffolds indicated the bioactivity of the composite fibers as a function of BG addition. Additionally, the presence of BG caused an increase in elastic modulus and a reduction in strength of fibrous scaffolds. A close match in terms of Young's modulus between composite fibers and native bone (15–100 MPa) was observed, confirming the intended application in bone regeneration. Similarly, the addition of BG (composition: 70 $\text{SiO}_2$ -25CaO-5 $\text{P}_2\text{O}_5$ ), concentration: 5, 10, and 15%(w/w) to poly (octane diol citrate) (POC) electrospun fibers demonstrated the potential interaction of BG (15%(w/w)) with the polymeric matrix through physical adsorption and carboxylate formation that led to increased glass transition temperature, elastic modulus, and mechanical strength as well as a decrease of the elongation at break.<sup>[49]</sup> In another related study, incorporating ascending concentrations of BG nanoparticles (composition: 76%  $\text{SiO}_2$ -18% CaO-6%  $\text{P}_2\text{O}_5$  (wt%), concentration: 5–40 wt%, size: 800 nm) in chitosan-PVA trilayer nanofibrous membranes indicated a string-like structure. Here, a low concentration of BG nanoparticles (5 and 10 wt%) enhanced yield strength and breaking strength but reduced the elongation. In contrast, a higher concentration of BG nanoparticles (20 and 40 wt%) decreased the tensile strength and percentage of elongation that originates from the introduction of stress concentrations by the addition of nanoparticles. In the case of biocompatibility, the addition of 40 wt% BG results in the best cell proliferation of fibroblast cells. Besides, the release of active ions from the BG particles demonstrated anti-inflammatory behavior and promoted angiogenesis.<sup>[50]</sup> In the investigation of Konyalı et al.,<sup>[51]</sup> ascending concentrations (1, 5, and 10 wt%) of silicate-based 13-93 BG

particles (in the micrometer range) and 13-93 BG short fibers (BGF) were incorporated into PCL to fabricate electrospun fibers for TE applications using acetone as a solvent. Increasing BG content led to progressively larger fiber diameters. Moreover, BG-containing fibers exhibited plate-like HA formation in SBF solution (30 days immersion), so that increasing BG content led to higher deposition of calcium phosphate layers. The fibrous meshes containing BGF showed overall less bioactivity when compared to the composite fibers containing BG particles. The authors also determined that both weight loss and silicon ion release were considerably increased (i.e., approximately 42% and 31%, respectively) for PCL fibrous meshes containing 10% BG particles when compared to those containing 10% of BG short fibers in the fibrous mesh (BGF). The authors attributed the difference in behavior between the two different inclusion types to morphological and dimensional characteristics as well as surface reactivity. In a recent investigation, Liverani et al.<sup>[52]</sup> fabricated homogeneous electrospun fibers exhibiting a shape memory effect using a benign solvent (glacial acetic acid). Such fibers are composed of triethoxysilane-terminated poly( $\epsilon$ -caprolactone) (PCL-TES) loaded with BG particles (composition: 45S5; concentration: 30 wt%; diameter: 2  $\mu\text{m}$ ). In this research, hydrolysis and condensation reactions between triethoxysilane groups of the polymer and the silanol groups that are present on the BG surface take place and thus lead to durable fibers by introducing additional cross-linking points. Also, BG particles support in vitro bioactivity and mineralization (formation of HA layers) after 7 days of immersion in SBF solution. Cell experiments demonstrated that the addition of BG particles did not negatively affect or inhibit the viability of ST-2 cells, which made the fibers good candidates for a range of biomedical applications.

#### 2.4. Bioactive Glasses Nanoparticles-Incorporated Fibers: In Vitro Aspects

The incorporation of nano-sized BG into polymeric matrices has attracted notable interest of the scientific community (Table 2).

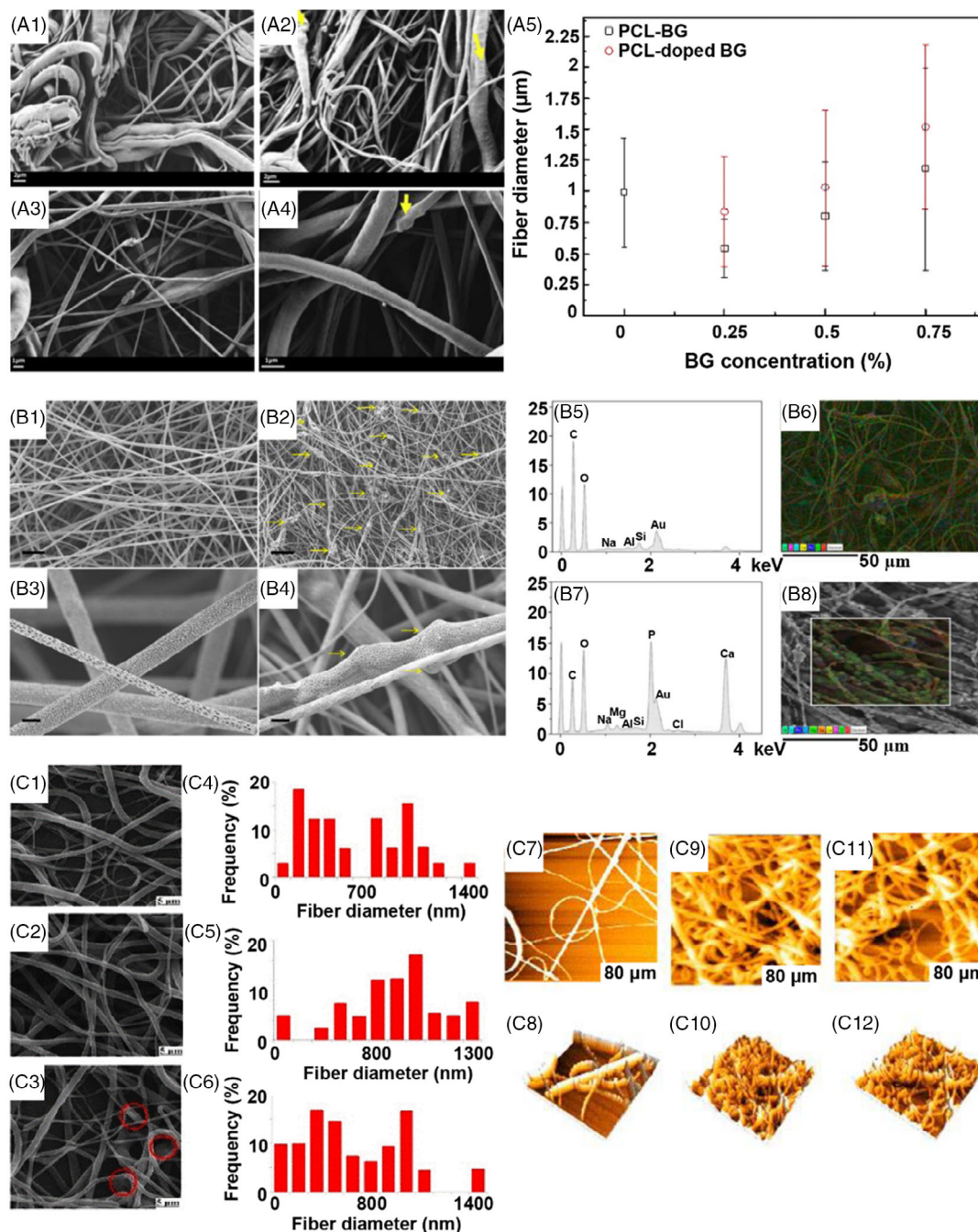


**Figure 3.** A1-A4) SEM micrographs of (A1-A2) PCL-BG and (A3-A4) PCL-doped BG fibers ((A1,A3) 0.25 wt% and (A2,A4) 0.75 wt% of BG). (A5) Size distribution of fiber diameter for different concentrations of BG. Reproduced with permission.<sup>[41]</sup> Copyright 2017, Elsevier. B1-B4) SEM micrographs of (B1,B3) PLLA and (B2,B4) PLLA-BG composite fibers with different magnifications. B6,B8) SEM images and B5,B7) EDS analysis of PLLA-BG fibers after (B5, B6) 7 days and (B7, B8) 21 days immersion in SBF solution. Reproduced with permission<sup>[47]</sup> under the open access Creative Common CC BY license. C1-C3) SEM micrographs, C4-C6) size distribution, and C7-C12) AFM image of PCL-chitosan fiber contains (C1,C4,C7,C8) 0 wt%, (C2,C5,C9,C10) 0.5 wt%, and (C3,C6,C11,C12) 1 wt% BG. Reproduced with permission.<sup>[58]</sup> Copyright 2019, SAGE Publications.

Nanometric BGs allow constructing scaffolds with improved mechanical behavior, surface roughness, hydrophilicity, and porosity.<sup>[53]</sup> These properties arise from the small size, high surface-area-to-volume ratio, and inherent physicochemical properties of nanoscale particles. The higher surface area enables the faster release of ions resulting in increased surface

reactivity and potentially enhanced protein adsorption, which is essential for cell attachment and subsequent cell behavior. Additionally, these structural features likely lead to faster mineralization of tissues like bone or teeth, which can be explained by the nanostructural properties of native bone tissue consisting of a mixture of collagen fibrils and HA nanocrystals.

**Table 2.** Summary of reviewed studies on BG nanoparticles-incorporated fibers.

Composition	BG features	Solvent	Doping ion	Application	Properties	References
PCL-gelatin-BG	Composition: 45% SiO <sub>2</sub> -25% CaO-25% Na <sub>2</sub> O-5% P <sub>2</sub> O <sub>5</sub>  Size: 10 nm  Concentration: 3 wt%	Formic acid	–	Bone TE	-4 times increase in fiber diameter as a function BG addition  -Biom mineralization of HA -Biocompatibility -High swelling ratio -High tensile strength and elongation	[56]
PLA-BG	Composition: 54% SiO <sub>2</sub> : 40% CaO : 6% P <sub>2</sub> O <sub>5</sub> (mol%)  Size: 27 nm Concentration: 5, 10, 20 wt%	Dichloromethane	–	Bone TE	-Increasing in fiber diameter as a function BG addition -Improving Young's modulus -Biom mineralization of HA -Viability of bone marrow-derived stromal cell line -Increasing alkaline phosphatase (ALP) expression	[57]
Chitosan-PCL-BG	Composition: composition: 61% SiO <sub>2</sub> -34% CaO-5% P <sub>2</sub> O <sub>5</sub> (wt%)  Size: 20–40 nm  Concentration: 0, 0.5, and 1.0 wt%	Chloroform-methanol	–	Cartilage TE	-Improvement in the cell–fiber interactions -Biocompatibility	[58]
SF-carboxymethyl cellulose-BG nanoparticles	Composition: 60% SiO <sub>2</sub> -36% CaO-4% P <sub>2</sub> O <sub>5</sub>  Size: 50–100 nm  Concentration: 10 and 20 wt%	Formic acid	–	Bone TE	-Increasing surface roughness -Improvement in cell proliferation and direct differentiation -Osteogenesis and Runx2/osteocalcin expression -Bone ECM formation	[63]
PCL-BG	Composition: 45S5  Size: 100 nm  Concentration: 5 wt%	Dichloromethane	–	Bone TE	-Increasing surface roughness  -Bioactivity	[64]
Chitosan-gelatin-BG	Composition 58S  Size: 67 nm Concentration: 2 wt%,	Acetic acid-water	–	Wound dressing	-Biocompatibility -Proliferation of dermal fibroblasts -Reduction in fiber diameter and increasing the porosity as a function of BG addition	[59]
Polyhydroxy butyrate-chitosan-BG nanoparticles	Composition: 41.04 gr SiO <sub>2</sub> , 29.25 gr CaO, 23.26 gr Na <sub>2</sub> O, and 1.78 gr P <sub>2</sub> O <sub>5</sub>  Size: 35–55 nm  Concentration: 7.5, 10, and 15 wt%	Trifluoroacetic acid	–	Bone and teeth TE	-Improvement in mechanical strength  -HA precipitation	[65]
nano HA-PCL-chitosan vs BG nanoparticles-PCL-chitosan	Composition: 45S5  Size: 20–80 nm  Concentration: 3 wt%	Formic acid-acetone	–	Bone and Periodontal TE	-Enhancing ALP activity  -Superior cell adhesion and proliferation	[35]

Furthermore, the surface bioreactivity of nanoparticles is higher than the one of micron-sized particles, and the resultant nanostructured surface features on scaffolds can induce improved osteoblast cell attachment.<sup>[15]</sup> It has also been

reported that electrospun scaffolds with nanofibrous architectures might promote angiogenesis, modulate macrophage and mast cell response, thereby affecting the secretion of vascular endothelial growth factor.<sup>[54,55]</sup>



The investigation by Elkhoully et al.<sup>[56]</sup> evaluated the effect of incorporated BG (composition: 45% SiO<sub>2</sub>-25% CaO-25% Na<sub>2</sub>O-5% P<sub>2</sub>O<sub>5</sub>, concentration: 3 wt%, size: 10 nm) in PCL-gelatin fibers. Choosing a “green” solvent (formic acid) made the fibers a suitable candidate for TE studies. According to this investigation, the addition of BG accompanies the formation of a bead-free structure, while an increase in diameter of electrospun fibers (more than 4 times) was observed. Deposition of HA on the fibers with a Ca/P ratio of 1.4 after a 14 day period in SBF solution was the other benefit of the composite fibers for hard tissue repair. Besides BG’s bioactive nature, a higher swelling ratio of BG-containing fibers affects their rapid mineralization.<sup>[50]</sup> Similarly, BG nanoparticles (composition: 54% SiO<sub>2</sub> : 40% CaO : 6% P<sub>2</sub>O<sub>5</sub> (mol%), size: 27 nm, concentration: 5, 10, 20 wt%) incorporated PLA fibers were investigated by Canales et al.<sup>[57]</sup> Agglomeration of the particles caused defects to increase with filler concentration. Using electrospun composite fibers with 5 and 20 wt% filler, the authors found that the presence of beads was most evident at concentrations greater than 10 wt%. An analysis of the pure PLA fibers revealed an average fiber diameter of 1.7 ± 0.6 μm. Values of the composite fibers involving 10 and 20 wt% of BG nanoparticles reached 2.8 ± 0.9 μm and 3.1 ± 0.8 μm, respectively, compared with neat PLA. It has been demonstrated that the presence of particles within fibers has a significant impact on Young’s modulus. Following 21 days of immersion in SBF solution, all composite fibers containing BG nanoparticles had developed bioactivity indicated by HA precipitation on the surface. Compared to pure PLA, the composites affected the bone marrow-derived stromal cell line viability and elevated ALP expression, indicating that the bone marrow-derived stromal cell line expressed an osteoblastic phenotype.

Although several studies have shown an increment in fiber diameter with the addition of BG, in research by Kandelousi et al.,<sup>[58]</sup> the diameter of chitosan-PCL fibers decreased, and surface roughness increased after the incorporation of nano-sized BG particles (composition: 61% SiO<sub>2</sub>-34% CaO-5% P<sub>2</sub>O<sub>5</sub> (wt%), size: 20–40 nm) (**Figure 3C1-C12**). Additionally, it was proven that the addition of nanoparticles causes a reduction in enthalpy of fusion compared to polymer fibers without BG addition due to rearrangement of the molecular structure. In this study, the change in enthalpy of fusion was shown to be accompanied by a reduction in Gibbs free energy leading to increasing reactivity of the fibers. An improvement in the interaction of composite fibers with human gingival fibroblast cells confirmed the biocompatibility of constructs and made them suitable for biomedical applications such as cartilage repair.<sup>[51]</sup> Similarly, Nosrati et al.<sup>[59]</sup> fabricated electrospun composite fibers composed of chitosan, gelatin, and BG nanoparticles (composition 58S, concentration: 2 wt%, size 67 nm). BG nanoparticles embedded in chitosan-gelatin scaffolds demonstrated biocompatibility, and dermal fibroblasts proliferated well on the composite fibers. When BG particles were incorporated into chitosan-gelatin fibers, a reduction in diameter could be attributed to the decreased viscosity of the fiber. The study found that the addition of BG nanoparticles slightly increased porosity, probably due to the smaller fiber diameters and wider void spaces in comparison with chitosan-gelatin fibers. To promote wound healing, it is recommended that porosity levels to be between 60% and 90% to enhance cell migration, ECM production, and gas exchange.

However, agglomeration of nanoparticles in composite fibers and poor dispersion homogeneity remain the main challenges related to the high surface energy of particles.<sup>[60]</sup> The homogeneous dispersion of BG nanoparticles is an important parameter that affects the bioactivity of the composite fibers as well as mechanical properties by preventing the polymeric chain movement.<sup>[61,62]</sup> Additionally, inhomogeneous nanoparticle dispersion may complicate the electrospinnability of solutions due to weak molecular interactions.

Nanofibrous silk fibroin (SF)-carboxymethyl cellulose scaffolds were incorporated with BG nanoparticles (composition: 60% SiO<sub>2</sub>-36% CaO-4% P<sub>2</sub>O<sub>5</sub>, size: 50 nm) to mimic the bone ECM. Here, the addition of BG nanoparticles increases the fiber diameter by increasing the viscosity of the solution. When the concentration of BG nanoparticles was set at 10 wt%, the particles were distributed along the fibers homogeneously. In comparison, increasing the BG content to 20 wt% affected fiber formation owing to the agglomeration of fine particles. The BG size was less than 50 nm, but agglomerates with a diameter of 100 nm were observed. At higher BG concentrations, fused fibers were observed that may originate from strong hydrogen and ionic bonding. It was observed that BG nanoparticle addition leads to wrinkles and increases surface roughness, positively affecting human mesenchymal stem cell attachment, proliferation, differentiation, and osteogenic ability. Herein, the composite fibers demonstrated dealkalization, calcium release, and the breakdown of Si-O-Si bonds within 7 days of culturing human mesenchymal stem cells (hMSCs). Accordingly, Ca and Si ions released during the dissolution led to gene activation.<sup>[63]</sup> Tamjid et al.<sup>[64]</sup> reported better distribution of BG nanoparticles (composition: 45S5) in PCL matrices with a particle size of less than 100 nm. Furthermore, the surface roughness of nanoparticles provided the conditions for the formation of HA crystals after 28 days in SBF solution. An investigation on polyhydroxy butyrate-chitosan-BG nanoparticles (composition close to 45S5 BG) electrospun fibers indicated uniform dispersion of particles (size: 35–55 nm) in the polymeric matrix. Appropriate BG dispersion in the polymeric matrix before electrospinning was achieved as well as possible chemical bonding at the BG-polymer interface. Here, BG nanoparticle concentration of 10 wt% showed electrospinnability and no agglomeration. Additionally, a tensile strength of 3.42 MPa was achieved with BG nanoparticle addition, a four times improvement over BG-free fibers. Moreover, composite fibers could adsorb calcium and phosphate ions to form HA-like layers after a 4 week immersion in SBF solution.<sup>[65]</sup>

## 2.5. Ion-Doped Bioactive Glass-Incorporated Fibers

It is well-known that doping BGs with trace metal ions, such as Ag<sup>+</sup>, Sr<sup>2+</sup>, Cu<sup>2+</sup>, Ce<sup>2+</sup>, Zn<sup>2+</sup>, and Co<sup>2+</sup>, induces special therapeutic functions enhancing their biological activity (**Table 3**).<sup>[66–69]</sup> Herein, tailored ion release kinetics should improve cell-fiber interaction, facilitate and increase osteogenesis, enhance angiogenesis, promote bioactivity, and/or induce anti-bacterial behaviour.<sup>[70,71]</sup>

It is expected that Zn-containing fibers have the potential to induce improved wound healing<sup>[72]</sup> and angiogenesis (given Zn ion biological activity).<sup>[73]</sup> Rajzer et al.<sup>[74]</sup> investigated the

**Table 3.** Influence of doping ions in BG chemical composition.

Ion	Influence	References
Ag	Inducing antibacterial activity	[17,119–121]
	Impressing biocompatibility	
	Reducing dissolution rate.	
	Inducing anti-inflammatory	
Zn	Higher surface area	[122–126]
	Bioactivity as a function of Zn ion concentration	
	Antibacterial effects	
	Production of ROS	
Mg	Anti-inflammatory	[127]
	Influence on bioactivity as a function of concentration	
Sr	Reduction in solubility	[128]
	Decreasing bioactivity	
Ce	Activation of superoxide	[129]
	Promoting antibacterial effects	
Al	Decreasing bioactivity	[130]
	Postponing dissolution	
Cu	Lipid peroxidation and protein oxidation effect	[131]
	Bacterial inhibition effect	
P	Decreasing bioactivity	[132]
Zr	Decreasing bioactivity	[133]

influence of BG addition (composition: 40% SiO<sub>2</sub>-54% CaO-6% P<sub>2</sub>O<sub>5</sub> (mol%), concentration: 2 and 4 wt%) on the morphology and diameter of PCL fibers (**Figure 4A1-A9**). According to the observations, large-sized particles (<45 μm) have a higher tendency to locate between the fibers while smaller ones (1 μm) are dispersed inside the fibers. Furthermore, a higher concentration of BG provided smaller fibers when the injection rate was set at 3 mL h<sup>-1</sup>. It was observed that by adding Zn-doped BG (composition: 49% CaO-5% ZnO-6% P<sub>2</sub>O<sub>5</sub>-40% SiO<sub>2</sub> (mol%), size: 1.5 μm) to PCL a larger fiber diameter could be achieved. The presence of Zn ions in the chemical composition of BG provides antibacterial properties to the fibers. In addition, ALP activity, an early indicator of osteoblast activity for bone regeneration, as well as osteogenic efficiency demonstrated higher levels in the fibers containing Zn-doped BG; however, ion incorporation did not affect cell morphology. Accordingly, Zn was introduced as a suitable ion to improve cell attachment and osteogenic differentiation of pre-osteoblasts and osteoblast-like cells.<sup>[66]</sup> In a parallel investigation by Neščáková et al.,<sup>[75]</sup> Zn-doped BG nanoparticles (composition: 84% SiO<sub>2</sub>-8% CaO-8% ZnO (mol%), size: ≈130–250 nm, concentration: 30 wt%) were incorporated in electrospun PCL fibers. Doping with Zn led to an increase in fiber diameter. Here, the experimental groups indicated the precipitation of HA-like layers however Zn-incorporated BGs led to a delay in biomineralization. Nontoxic degradation by-products for murine stromal cells indicated the possibility of Zn-doped fibers for TE and drug delivery applications.

The incorporation of BG particles (composition: 45S5, size: <20 μm, concentration: 20 wt%) in chitosan-polyethylene oxide

solution showed a slight increase in electrospun fiber diameter although the difference was not significant. Here, doping Zn in the BG composition led to a reduction in fiber diameter.<sup>[42]</sup> Similar research results were reported by Saatchi et al.<sup>[76]</sup> for the electrospinning of chitosan-polyethylene oxide fibers containing cerium-doped BG particles (composition: 60% SiO<sub>2</sub>-28% CaO-4% P<sub>2</sub>O<sub>5</sub>-8% Ce<sub>2</sub>O<sub>3</sub> (mol%), size: 35 nm) at different concentrations (10–40 wt%). They found that the highest concentration of cerium-doped BG led to a significant size distribution of fibers (50–500 nm) due to the agglomeration of nanoparticles. In this regard, electron microscopy images proved the presence of submicron clusters in the fibers. A higher concentration of cerium-doped BG indicated better cytocompatibility and enhanced cell adhesion and spreading by providing rough nanofiber surfaces. It was shown that the enhanced agglomerate formation did not restrict the cellular response. Additionally, cell proliferation was observed across the network with a three-dimensional shape. Malekahmadi et al.<sup>[77]</sup> developed PCL-gelatin-Cu doped BG (composition: 45% SiO<sub>2</sub>-24.5% Na<sub>2</sub>O-23.5% CaO-6% P<sub>2</sub>O<sub>5</sub>-1% CuO (wt%), size <100 nm, concentration: 1 (wt%)) fibers. Upon the incorporation of gelatin and CuBG particles, the wettability, pore size, and Young's modulus of the PCL electrospun fibers significantly improved. The growth of bone marrow-derived mesenchymal stem cells on PCL-gelatin-CuBG composite fibers with the least attachment took 7 days to reach confluence. Long-term hypoxia responses and cell death were not observed following the slow release of copper ions from scaffolds. Additionally, the authors hypothesized that a trace amount of copper combined with PCL-gelatin might benefit periodontal regeneration. In a recent study, Akturk et al.<sup>[78]</sup> investigated the influence of the incorporation of BG nanoparticles (composition: 45S5 BG, concentration: 10, 15, and 20 5(w/w), size: 45 μm) and copper metal nanoparticles (2.5, 5, 7.5%(w/w)) in electrospun PCL fibers for TE applications. Here, BG addition led to increased cytocompatibility, while toxicity increased as a function of increasing copper content. This study demonstrated the biocompatibility of fibers (tested with L929 fibroblasts cells) when the content of the BG phase was set at 15% w/w while 0.025% w/w was the concentration of copper nanoparticles. Twenty-eight days of immersion in SBF indicated stability and mineralization of the fibers, proving their osteogenic potential. At the same time, copper ion release should positively affect the angiogenic potential of the fibers.

An investigation by Moura et al.<sup>[41]</sup> on PCL-BG fibers indicated that doping cobalt and silver in BG (composition: SiO<sub>2</sub>:CaO:P<sub>2</sub>O<sub>5</sub>:CoO:Ag<sub>2</sub>O (mol%) = 50:40:5:2.5:2.5, size: 32 ± 17 nm) might enhance the angiogenic performance and induce antibacterial features to composite scaffolds, improving tissue regeneration. In a similar approach, embedding PCL fibers with 15 wt% boron, cobalt, and dual boron/cobalt co-doped BG nanoparticles (BG composition: 80% SiO<sub>2</sub>-20% CaO (mol%), size: 457 ± 20 nm; B5Co2 composition: 73% SiO<sub>2</sub>-20% CaO-5% B<sub>2</sub>O<sub>3</sub>-2% CoO (mol%), size: 361 ± 9 nm; B10Co4 composition: 66% SiO<sub>2</sub>-20% CaO-10% B<sub>2</sub>O<sub>3</sub>-4% CoO (mol%), size: 331 ± 21 nm) was investigated by Chen et al.<sup>[79]</sup> for promoting vascularization. Acetic acid was used as a benign solvent for green electrospinning. Here, the scaffolds showed biocompatible behavior after culturing bone marrow-derived stromal cells (ST-2 cell line). Besides, doping with boron and cobalt

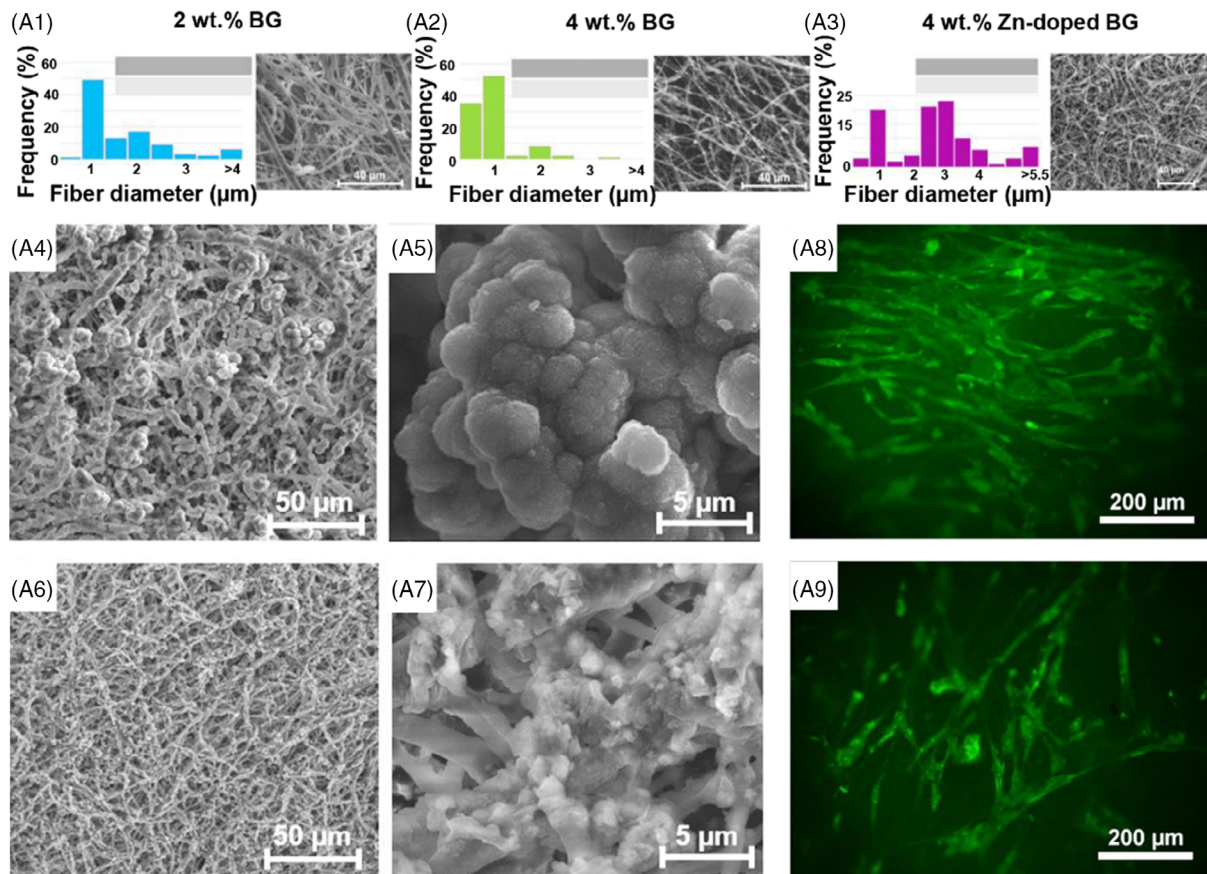


**Figure 4.** A1-A3) Size distribution and corresponded FESEM micrographs of (A1) PCL-2 wt% BG, (A2) PCL-4 wt% BG, and (A3) PCL-4 wt% Zn-doped BG scaffolds. A4-A7) FESEM micrographs with a different magnification of (A4,A5) PCL-BG, and (A6,A7) PCL-Zn-doped BG scaffolds after a 7 day immersion in the SBF solution. A8,A9) Fluorescence microscopy images of osteoblasts on (A8) PCL-BG and (A9) PCL-Zn-doped BG scaffolds after a 14 day culture. Reproduced with permission<sup>[74]</sup> under the open access Creative Common CC BY license.

simultaneously led to vascular endothelial growth factor secretion, increasing angiogenic potential. Erbium and terbium co-doped BG particles ( $\text{Er}^{3+}$  and/or  $\text{Tb}^{3+}$ -doped 13-93 BG particles, size: 1.45–3.57  $\mu\text{m}$ ) were incorporated in PVA fibers in the investigation of Deliormanlı et al.<sup>[80]</sup> Doping such ions did not inhibit the bioactivity of the BG and induced green luminescent behavior to BG, making the BG suitable for TE and bioimaging studies. Duan et al.<sup>[81]</sup> fabricated electrospun fibers composed of polyurethane, SF, and BG (concentration: 0.4% (wt/vol)). Here the addition of BG led to excellent mechanical properties with tensile strength reaching 14.6 MPa (pure silk film: 3.8 MPa) and tensile strain reaching 70% (pure silk film: 7.9%). It was also shown that fibers containing BG had superior hydrophilicity, which led to PU (97.3°) and silk fiber membrane (77.4°) contact angles reaching 39.2° and 35.9° after the addition of BG, respectively. CCK-8 analysis using bone marrow mesenchymal stem cells confirmed the biocompatibility of the composite fibers. Besides, Si and B ions release indicated a positive influence on ALP activity, osteogenesis, and bone repair, making the fiber suitable for bone TE applications.

Strontium borosilicate BG (composition:  $0.05\text{Na}_2\text{O} \cdot x\text{MgO} \cdot \gamma\text{CaO} \cdot (0.35-x-\gamma) \text{SrO} \cdot 0.20\text{B}_2\text{O}_3 \cdot 0.40\text{SiO}_2$  (molar ratio, where  $x, \gamma = 0.35$  or  $0.00$ , and  $x \neq \gamma$ ), concentration: 10% (w/w),

size:  $<45 \mu\text{m}$ ) was incorporated in a PLLA electrospun membrane for bone TE application. Results indicated homogeneous distribution of BG particles in the polymeric fibers so that strontium borosilicate BG addition increased water uptake and degradation rate. Besides, BG particle addition enhanced the mechanical properties (69% higher Young's modulus and 36% higher tensile strength). Moreover, the osteogenic differentiation of bone marrow-derived mesenchymal stem cells was improved as a function of strontium borosilicate BG addition. Particle-containing membranes demonstrated upregulated osteogenic gene expression as well as increased ALP secretion.<sup>[82]</sup> **Table 4** summarizes relevant studies on ion-doped BG-containing electrospun composite fibers.

## 2.6. Advanced Biological Evaluation of Bioactive Glass-Containing Electrospun Fibers in Hard Tissue Engineering

Cell-scaffold interaction plays a remarkable role in determining the success of TE strategies. It refers to cell adhesion to biomaterials through adhesion proteins, including fibronectin, collagen, laminin, and vitronectin, using specific cell receptors, which will affect cell behavior such as proliferation, migration,

**Table 4.** Summary of reviewed studies on ion-doped BG-containing electrospun composite fibers.

Composition	BG features	Solvent	Doping ion	Application	Properties	References
PCL-BG	Composition: 40% SiO <sub>2</sub> -54% CaO-6% P <sub>2</sub> O <sub>5</sub> (mol%) Size: <45 μm Concentration: 2 and 4 wt%	Chloroform-methanol	Zinc	Nasal TE	-Antibacterial properties -ALP activity -Osteogenic performance	[74]
PCL-BG	Composition: 84% SiO <sub>2</sub> -8% CaO-8% ZnO (mol%) Size: ≈130–250 nm Concentration: 30 wt%	Acetic acid	Zinc	Drug delivery and TE	-Increasing in fiber diameter -HA-like layers precipitation -Zn-incorporated BGs indicated a delay in biomineralization -Non-toxic degradation by-products	[75]
Chitosan-polyethylene oxide-BG	Composition: 60% SiO <sub>2</sub> -28% CaO-4% P <sub>2</sub> O <sub>5</sub> -8% Ce <sub>2</sub> O <sub>3</sub> (mol%) Size: 35 nm Concentration: 0, 10, 20, 30, and 40 wt%	Acetic acid	Cerium	Soft TE	-Cytocompatibility -Enhancing cell adhesion and spreading	[76]
PCL-gelatin- BG	Composition: 45% SiO <sub>2</sub> -24.5% Na <sub>2</sub> O-23.5% CaO-6% P <sub>2</sub> O <sub>5</sub> -1% CuO (wt%) Size <100 nm concentration: 1 wt%	1,1,1,3,3,3-Hexafluoro-2-propanol	Copper	Periodontal tissue	-Improvement of wettability, pore size, and Young's modulus as a function of BG addition -No sign of long-term hypoxia responses and cell death -Postponing cell growth	[77]
PCL-BG-Copper	Composition: 45S5 Size: 45 μm Concentration: 10, 15, and 20 5(w/w)	Dichloromethane: dimethylformamide (80:20)	–	TE	-Increasing cytocompatibility as a function of BG addition -Mineralization ability in the SBF solution -Osteogenic potential	[78]
PCL-BG	Composition: SiO <sub>2</sub> :CaO:P <sub>2</sub> O <sub>5</sub> :CoO:Ag <sub>2</sub> O (mol%) = 50:40:5:2.5:2.5 Size: 32 ± 17 nm Concentration: 0.25–0.75 wt%	Acetone	Cobalt and silver	Wound healing	-Enhancing angiogenic performance -Inducing antibacterial features	[41]
Chitosan-polyethylene oxide-BG	Composition: 45S5 Size: <20 μm Concentration: 20 wt%	Aqueous acetic acid	Zinc	Wound healing	-Reduction in fiber diameter as a function of Zn	[42]
PCL-BG	BG nanoparticles, Composition: 80% SiO <sub>2</sub> -20% CaO (mol%), size: 457 ± 20 nm B5Co2 nanoparticles, Composition: 73% SiO <sub>2</sub> -20% CaO-5% B <sub>2</sub> O <sub>3</sub> -2% CoO (mol%), size: 361 ± 9 nm, B10Co4 nanoparticles, Composition: 66% SiO <sub>2</sub> -20% CaO-10% B <sub>2</sub> O <sub>3</sub> -4% CoO (mol%), size: 331 ± 21 nm Concentration: 15 wt%	Acetic acid	Boron and cobalt	Soft TE	-Promoting vascularization -Biocompatible -Increasing angiogenesis potential	[79]
PVA-BG	Composition: Er <sup>3+</sup> and/or Tb <sup>3+</sup> -doped 13-93 BG particles Size: 1.45–3.57 μm	Ethanol	Erbium and terbium	TE and bioimaging	-Green luminescent behavior	[80]
Polyurethane-silk fibroin-BG	Concentration: 0.4% (wt/vol)	Hexafluoroisopropanol	Boron	Bone repair	-Excellent mechanical properties and superior hydrophilicity as a function of BG addition -Biocompatibility	[81]



**Table 4.** Continued.

Composition	BG features	Solvent	Doping ion	Application	Properties	References
PLLA-Strontium borosilicate BG	(Composition: $0.05\text{Na}_2\text{O}\cdot x\text{MgO}\cdot y\text{CaO}\cdot (0.35-x-y)\text{SrO}\cdot 0.20\text{B}_2\text{O}_3\cdot 0.40\text{SiO}_2$ (molar ratio, where $x, y = 0.35$ or $0.00$ , and $x \neq y$ ), Concentration: 10% (w/w), Size: $<45\ \mu\text{m}$ )	Dichloromethane	Strontium	Bone TE	-Si and B ion release indicated a positive influence on ALP activity, osteogenesis -Homogeneous distribution of BG particles in polymeric fibers -Increasing water uptake and degradation rate as a function of BG addition -Increasing mechanical properties (69% higher Young modulus and 36% higher tensile strength) in composite fibers -Osteogenic differentiation of the bone marrow-derived mesenchymal stem cells -Upregulation of osteogenic gene expression (Alpl, Sp7, and Bglap) as well as ALP secretion	[82]

differentiation, and specific cell functionalities.<sup>[83]</sup> Here, one of the critical physical properties of electrospun scaffolds is surface wettability since it directly affects the interaction with proteins and cells. In this regard, the addition of BG particles to polymer fibers increases their wettability. BG-containing composite fibers can provide desirable interaction with water molecules as well as exhibiting surface nano roughness, both of which are necessary for the improvement of cell growth, migration, proliferation, and differentiation.<sup>[58]</sup> Additionally, the incorporation of BG particles (composition:  $70\text{SiO}_2\cdot 25\text{CaO}\cdot 5\text{P}_2\text{O}_5$ , concentration: up to 10 wt%) inside PLA electrospun fibers led to in vitro HA precipitation as well as improved osteoblastic cell adhesion and growth, suggesting the application of the composite fibers in hard tissue regeneration.<sup>[84]</sup> A similar investigation by Ding et al.<sup>[85]</sup> on BG (composition: 58S, concentration: 0–16.7 wt%) incorporated ultrathin polyhydroxybutyrate (PHB)-PCL fibers indicated suitable adhesion and viability of MG-63 cells as well as increased expression of ALP and higher mineral calcium nodule content in BG-containing fibers.

Shamsi et al.<sup>[86]</sup> fabricated PLLA-BG (composition: 89%  $\text{SiO}_2$ -8%  $\text{CaO}$ -3%  $\text{P}_2\text{O}_5$  (wt%)) composite fibers for bone repair. The incorporation of BG nanofibers in composite scaffolds and resultant  $\text{SiO}_2$  release could improve bone marrow mesenchymal stem cell attachment, growth, proliferation, as well as calcium phosphate deposition after 14 days. The expression of ALP, osteocalcin, osteopontin, collagen I, and Runt-related transcription factor 2 (RUNX2) furthermore confirmed the osteogenic performance of BG-loaded constructs.

Electrospun PCL fibers incorporated with BG particles (composition: 5%  $\text{SiO}_2$ ; 24.5%  $\text{CaO}$ ; 24.5%  $\text{Na}_2\text{O}$ ; and 6%  $\text{P}_2\text{O}_5$ , concentration: 10 wt%) were fabricated for bone regeneration.<sup>[87]</sup> The in vitro bioactivity experiment indicated that the addition of BG into PCL fibers affected nucleation of the apatite layer since mineralization nodules were detected after culturing mesenchymal stem cells (MSCs) in a nonosteogenic medium.

Additionally, BG-containing fibers supported osteogenic differentiation of MSCs, indicating the bioactivity of the composite fibers. Implantation of scaffolds in twenty-four male rats showed a large amount of newly formed trabecular bone.

Since the biocompatibility of composite fibers is a crucial property, Lian et al.<sup>[49]</sup> focused on the biological behavior of composite fibers composed of poly (octane diol citrate)-BG composite (composition: 76%  $\text{SiO}_2$ -18%  $\text{CaO}$ -6%  $\text{P}_2\text{O}_5$  (wt%), concentration: 5–40 wt%, size: 800 nm). Here, electrospun fibers were found to stimulate the growth of mouse bone marrow mesenchymal stem cells, ALP activity, and mineralization (Figure 5A1,A2). Moreover, the expression of collagen type I and osteocalcin and osteogenic differentiation were promoted in BG-containing fibers, making them suitable candidates for bone regeneration.

Bilayered electrospun fibers composed of PVA and SF were incorporated with BG nanoparticles (composition: 60%  $\text{SiO}_2$ -36%  $\text{CaO}$ -4%  $\text{P}_2\text{O}_5$ , size:  $<100\ \text{nm}$ ) in the investigation of Singh et al.<sup>[88]</sup> (Figure 5B3-B9)). The composite fibers showed suitable stiffness, hydrophilicity, as well as superior bioactivity. The cellular study confirmed excellent mesenchymal stem cell attachment, spreading, proliferation, and osteogenic differentiation. Besides the formation of bone-like nodules, an increased ALP activity and osteocalcin expression, as well as biomineralization, are the advantages of BG addition to polymeric fibers. As mentioned above, the release of inorganic ions such as Si, Ca, and P can be exploited for the differentiation of stem cells to the osteogenic lineage.

Biomimetic collagen-chitosan-BG (composition: Si/Ca/P = 80:15:5 mole ratio) nanofibers were evaluated in research conducted by Zhou et al.<sup>[89]</sup> to understand the potential of composite fibers on inducing periodontal TE. They observed that composite fibers could increase human periodontal ligament cell viability and osteogenic gene expression as well as improving expression of RUNX2 and osteopontin protein. Implantation

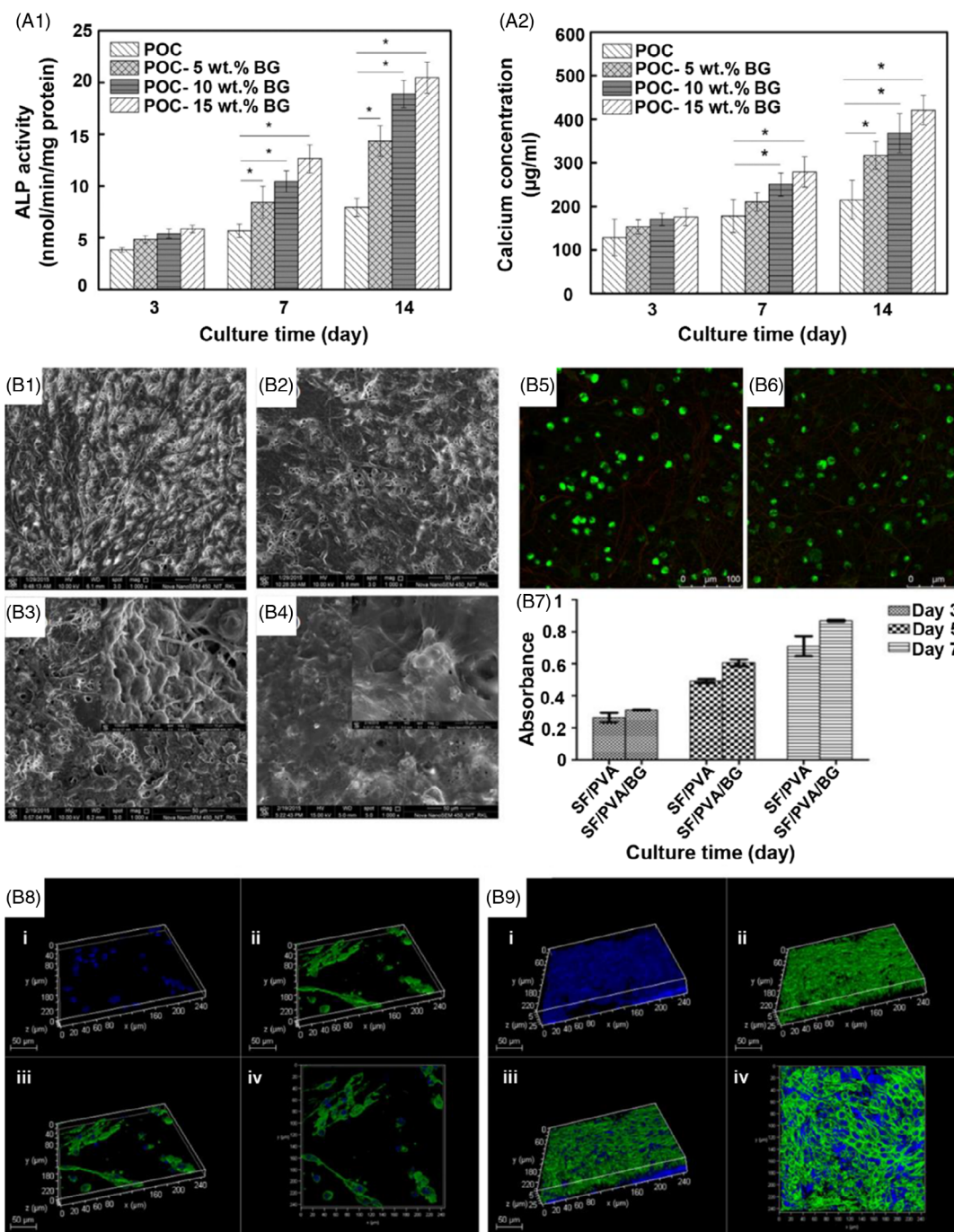


**Figure 5.** A1) ALP activity A2) calcium content of the mesenchymal stem cells after a 3, 7, and 14 day culture on poly (octanediol citrate) (POC) and POC-BG with ascending concentration of BG (\* $p < 0.05$ ). Reproduced with permission.<sup>[49]</sup> Copyright 2018, Elsevier. B1-B4) FESEM micrographs of (B1, B3) SF-PVA and (B2, B4) SF-PVA-BG scaffolds after a 7 and 14 day culturing period of mesenchymal stem cells. B5, B6) live-dead cell staining after culturing the mesenchymal stem cells on (B5) SF-PVA and (B6) SF-PVA-BG scaffolds, and B7) MTT results of cell viability as a function of time. B8, B9) Confocal images for cytoskeleton of mesenchymal stem cells after a 14 day culture on (B8) SF-PVA and (B9) SF-PVA-BG scaffolds. Reproduced with permission.<sup>[88]</sup> Copyright 2017, IOP Publishing Ltd.

of BG-containing constructs in a dog class II furcation defect model demonstrated improved bone formation and mineralization. In a recently published study, El-Okaily et al.<sup>[90]</sup> fabricated risendronate sodium-loaded composite fibers based on PVA and chitosan that were incorporated with BG nanoparticles

(composition: 46 % SiO<sub>2</sub>, 24 % CaO, 24 % Na<sub>2</sub>O, and 6 % P<sub>2</sub>O<sub>5</sub> (wt%); concentration: 10–50 wt%; and size: 5.9–13.7 nm) for bone TE application. Electrospun fibers possessed a homogeneous, uniform, and dense microstructure with fiber diameters in the range of 20–125 nm. According to the obtained results, the

addition of BG nanoparticles retarded the drug release profile of the model osteoporotic drug as well as increasing overall drug release efficiency significantly, thus the scaffolds hold potential as sustained drug release carriers. The drug release was found to take place through a two-stage intraparticle diffusion mechanism.<sup>[79]</sup>

Gelatin-BG (composition: 70% SiO<sub>2</sub>-25% CaO-5% P<sub>2</sub>O<sub>5</sub> (mol%), size: ≈3 μm) composite fibers were developed, which exhibited a bead-free microstructure that supported the formation of multicellular layers, osteoblastic MC3T3-E1 cell ALP activity, and mineralization during in vitro culture.<sup>[91]</sup> Increasing human keratinocyte adhesion and enhanced secretion of collagen type I and vascular endothelial growth factor by human dermal fibroblasts were observed in BG (composition: Si/Ca/P = 80:15:5 molar ratio) incorporated collagen fibers. Also, collagen-BG nanofibers accelerated rat skin wound healing with adequate mechanical strength.<sup>[92]</sup> Similarly, BG (composition: 70S) addition to SF fibers improved the MG-63 osteoblast cellular performance by providing a hydrophilic structure. Increasing ALP activity indicated the potential of the fibers for regeneration of osteochondral tissue.<sup>[93]</sup>

In parallel studies, Hashemi-Beni et al.<sup>[94]</sup> focused on cell–fiber interactions using poly hydroxyl butyrate-chitosan electrospun fibers incorporated with BG nanoparticles (45S5 composition, size: 35–55 nm). The obtained results indicated nontoxicity of the fibers and appropriate cell adhesion and proliferation. Moreover, flow cytometric analysis showed that isolated cells from the pulp of deciduous teeth were positive for mesenchymal CD90 and CD146 markers, while they were negative for hematopoietic CD14 and CD19 markers. This research was continued by Khoroushi et al.,<sup>[95]</sup> and the results demonstrated that the composite fibers supported proliferation and differentiation of human exfoliated deciduous teeth stem cells. Their observation indicated a sixfold enhancement in dentin sialophosphoprotein gene and collagen-type I expression, and a twofold enhancement in ALP activity.

In a related study, composites comprising PCL and 58S BG (size: 38 μm, 5 wt%) were fabricated using electrospinning for applications in bone regeneration (Figure 6A1–A4). Composite fibers presented a suitable potential for HA formation after 21 days soaking in SBF solution. Furthermore, culturing with dental pulp stem cells exhibited cell adhesion and proliferation as well as matrix mineralization, arising from the BG particle addition to polymer fibers, which also improves hydrophilicity, surface roughness besides providing cell anchorage sites.<sup>[96]</sup>

“F18” BG (size: 5 μm)-PCL (1:18 weight ratio) composite fibers were studied by Pitaluga et al.<sup>[97]</sup> for small-sized bone injury treatment by guided TE technique. The addition of BG to PCL fibers increased the tensile strength, but there were no significant differences recognized in terms of cytotoxicity and MG-63 cell proliferation within 14 days. However, ALP activity after a 14 day incubation period of MG-63 cells in fiber-containing media showed a significant increase in ALP level, exhibiting outstanding osteogenic performance.<sup>[86]</sup>

The development of composite fibers composed of SF-carboxymethyl cellulose confirmed the positive role of BG nanoparticles (composition: 60% SiO<sub>2</sub>-36% CaO-4% P<sub>2</sub>O<sub>5</sub> (mol%), size: 50 nm) resulting from the released Ca and Si ions on viability, adhesion, and proliferation of human mesenchymal stem

cells.<sup>[63]</sup> Direct osteogenic differentiation was proven by determining ALP activity as well as Runx2/osteocalcin expression. In addition, the synthetic matrix supported bone ECM formation, which is essential in the bone regeneration process.

Incorporation of 15 wt% BG particles (composition: standard 45S5 BG, size: 10–20 μm) in chitosan-polyethylene oxide nanofibers indicated that BG-containing fibers could improve biomineralization as well as expression of osteocalcin and osteopontin after SaOS-2 human osteosarcoma cell line culture, confirming the ability of the composite fibers to stimulate osteoblasts to secrete bone ECM.<sup>[46]</sup>

In related research, copper-doped 45S5 BG particles (composition: 45% SiO<sub>2</sub>-24.5% Na<sub>2</sub>O-6% P<sub>2</sub>O<sub>5</sub>-22% CaO-2.5% CuO (wt%), size: 4 μm, concentration: 2, 4, and 9 wt%) were embedded in electrospun zein fibers (Figure 6B1–B12). Herein, BG addition reduced Young’s modulus and ultimate tensile strength values compared to those of BG-free fibers. Also, copper-containing BGs exhibited antibacterial activity after culturing *Staphylococcus aureus* and *Escherichia coli* bacteria. Osteogenic and angiogenic ability of the BG-containing fibers led to an increase in the number of MG-63 (bone osteosarcoma cell line) and C2C12 (mouse myoblast cell line) cells, making composite polymer fibers suitable candidates for TE applications.<sup>[98]</sup>

Multifunctional bone-like membranes were fabricated by a combination of BG and collagen. According to observations, hollow BG fibers (composition: 46.13% SiO<sub>2</sub>-24.35% Na<sub>2</sub>O-26.91% CaO-2.6% P<sub>2</sub>O<sub>5</sub> (mol%), size: 240 nm) exhibited hydrophilicity (water drop contact angle 75°) and optimal bioactivity. The membranes showed superior mechanical properties so that the Young’s modulus and ultimate tensile strength ranged between 126 and 173 MPa and 1.18–1.95 MPa, respectively. Cellular investigation with fibroblast cells (3T3) resulted in improved cell adhesion and proliferation as well as cell orientation. Besides, the enhanced osteogenic performance of the membranes was confirmed by determining ALP activity and by alizarin red staining of osteoblast cells. The presence of BG led to an increase in the level of expressed Runx2, collagen type I, mRNA, osteocalcin, and osteonectin, which are essential markers in bone regeneration. Moreover, the vascularization in the chick chorioallantoic membrane model proved the potential of the membranes for bone repair.<sup>[99]</sup>

One issue encountered in electrospun biopolymer-BG fibers depending on the characteristics of the polymer matrix is the “masking” of the BG fillers by the polymer matrix, thereby reducing the fiber bioactivity. One method to address this was presented in a recent study by Abdal-hay et al.,<sup>[100]</sup> who developed a fabrication method to assemble ordered and aligned arrays of BGC “nanoneedle-like structures” on the outer surface of three different polyamide 6 (PA6) substrates fabricated using film casting, 3D printing filaments and electrospinning, respectively, for applications in bone TE. Akermanite bioactive (Ca<sub>2</sub>MgSi<sub>2</sub>O<sub>7</sub>) powder was used, which was prepared using sol–gel with particle sizes ranging between 2 and 30 μm. The aligned arrays of nanoneedles were applied to the electrospun PA6 fiber mats after electrospinning using a hydrothermal process at 150 °C and saturated vapor pressure, which led to uniformly coated PA6 fiber mats. Cell studies demonstrated very high proliferation, viability, and spreading of MC3T3 cells. Furthermore, osteogenic



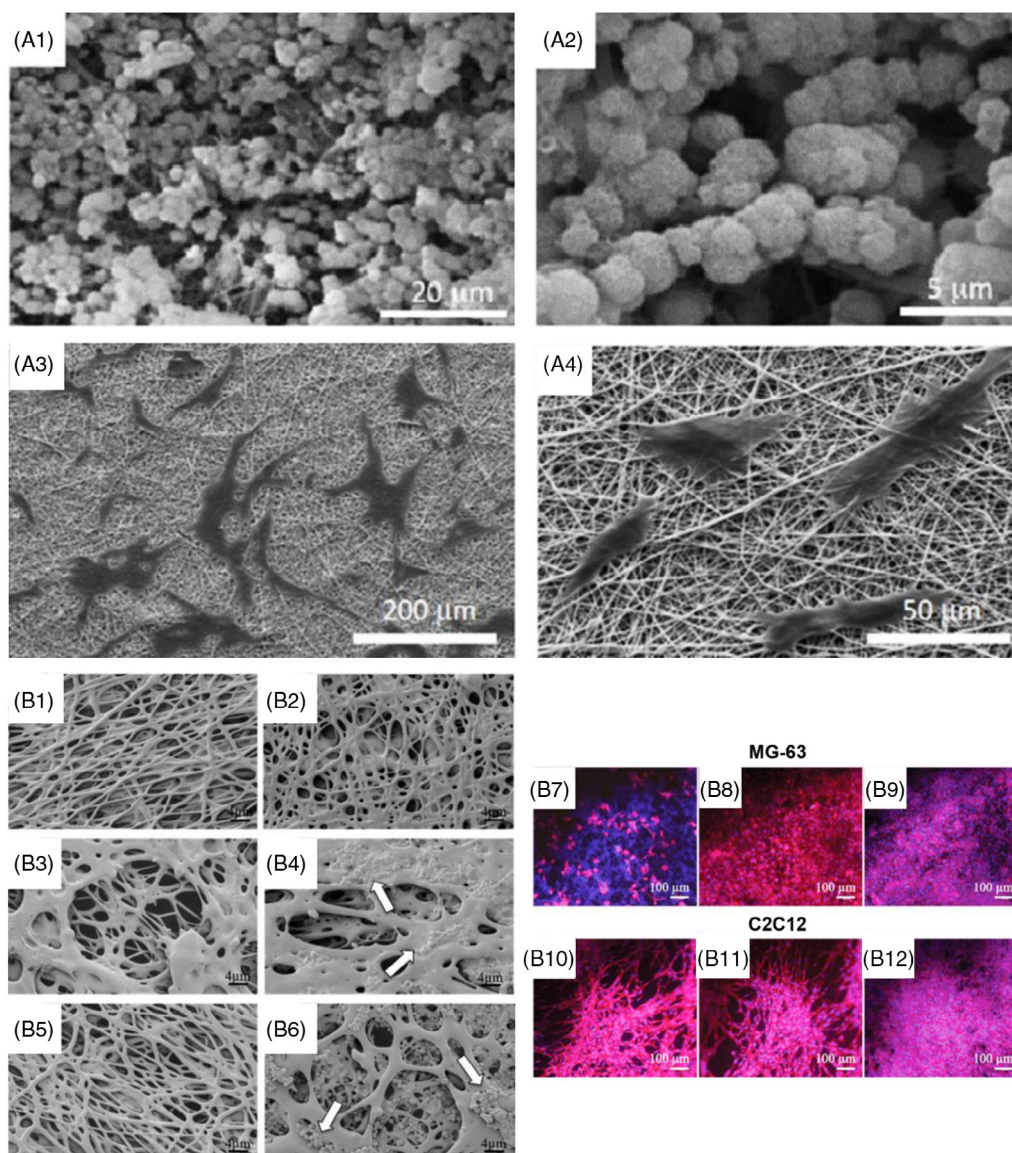


**Figure 6.** A1,A2) SEM micrographs of PCL-BG composite fibers after a 21 day immersion in SBF solution with different magnification. A3,A4) SEM micrographs of PCL-BG composite fibers after a 24 h culture of dental pulp stem cells with different magnification. Reproduced with permission<sup>[96]</sup> under the open access Creative Common CC BY-NC-ND license. B1-B6) SEM micrographs of (B1,B2) zein, (B3,B4) zein-BG, and (B5,B6) zein-copper-doped BG fibers after (B1,B3,B5) 1 day and (B2,B4,B6) 7 days biodegradation in Eagle's minimal essential medium. The white arrows are indicators of HA crystal formation in BG-containing fibers. B7-B12) Fluorescence microscope images of (B7-B9) MG-63 and (B10-B12) C2C12 cells in (B7,B10) zein, (B8,B11) zein-BG, and (B9,B12) zein-copper-doped BG fibers after 3 days of culture. All the images are shown at 10× magnification. Reproduced with permission<sup>[98]</sup> under the open access Creative Common CC BY-NC-ND license.

differentiation and accelerated expression of late osteoblast marker genes were observed for the BGC-coated fiber meshes compared to the uncoated control group. The composite fibers also showed a large degree of apatite formation during incubation in physiological solution. Thus, the study demonstrated a method for in situ immobilization of BG nanoneedles leading to favorable cell behavior, which may be applied to other polymer substrates.

Tabia et al.<sup>[101]</sup> fabricated fibrous membranes composed of PCL and nanoscaled BG (nanoparticle composition: 85% SiO<sub>2</sub>,

12% CaO, and 3% MgO (wt%), synthesized by the Stöber process) using green electrospinning (using glacial acetic acid as a solvent). The fibrous membranes were fabricated using cetyl trimethyl ammonium bromide (CTAB) as a template. The composite structures thus fabricated were proposed as barrier membranes for guided bone regeneration, which is one of the strategies used in dental implantology to augment bone volume. The nBG particles had an average diameter of 300 nm, and three different BG contents were studied in this work, i.e. 5, 10, and 15% by weight. The content of nBG used was found to be a



determining factor for adjusting alignment, uniformity, biodegradability, and bioactivity of the PCL fibers. For 5 wt%, the PCL/BGn composite fibers showed enhanced wettability but only poor to moderate degradability and bioactivity. However, for 10% and 15 wt% nBG content, very high in vitro biomineralization was observed. The rate of degradation was found to match the rate of HA deposition. The nBG particles were dispersed homogeneously within the fibrous PCL matrix. For the proposed application as a barrier membrane, the PCL/nBG composite fibrous membranes were proposed to be advantageous in comparison to the current gold standard of using nondegradable PTFE membranes, which require subsequent surgical removal.

Electrospun PCL-BG scaffolds (composition: 60% SiO<sub>2</sub>, 36% CaO, and 4% P<sub>2</sub>O<sub>5</sub> (mol%), concentration: 20 (wt%)) were fabricated using BG nanofibers (BGNFs, 450 nm) and compared to an existing composite fabricated using BG microparticles (BGPs, 4 μm). According to the results, the incorporation of BGNFs in polymeric scaffolds further enhanced the stiffness of the composite. According to in vitro experiments using the MC3T3 cell line, BGNF-containing scaffolds demonstrated better biocompatibility over BGP-containing ones. A significant difference between the PCL-BGNF fibers and PCL-BGP ones was found in terms of bioactivity in a physiological environment. In addition, the in vivo experiments with Sprague-Dawley albino rats demonstrated that the PCL/BGNF composite could successfully regenerate bone when implanted in calvarial defects.<sup>[102]</sup>

### 2.7. Advanced Biological Evaluation of Bioactive Glass-Containing Electrospun Fibers in Wound Healing and Skin Repair

One of the challenging issues in skin TE is the formation of vascularized networks in wounded tissues.<sup>[103]</sup> It is well known that Ca and Si in BG compositions, when present in specific concentration, promote angiogenesis.<sup>[79,104]</sup> Si ions have indicated a strong potential to upregulate the expression of hypoxia-inducible factor-1 $\alpha$ , and as a result, upregulate the expression of proangiogenic factors, including fibroblast growth factors and vascular endothelial growth factors.<sup>[105]</sup> Beyond that, Ca showed the potential to promote wound healing by regulating vasodilation.<sup>[106]</sup>

Accordingly, BG nanoparticles (composition: 60% SiO<sub>2</sub>-36% CaO-4% P<sub>2</sub>O<sub>5</sub> (mol%), size: 100 nm) were incorporated in PCL-collagen electrospun fibers for soft tissue repair. Results indicated the crucial influence of BG particles in the wound-healing process because of the improvement in expression of CD31, vascular endothelial growth factor, and hypoxia-inducible factor 1- $\alpha$ , as well as collagen type III deposition, which are signs of increased angiogenesis and suitable wound healing.<sup>[107]</sup>

Electrospun PCL-BG (composition: 77S, size: 300–710 μm, concentration: 0–8 wt%) composite fibers developed by Lin et al.<sup>[108]</sup> indicated a potential application for skin TE. Ascending concentration of BG led to a reduction in fiber diameter. However, higher BG loading was found to negatively affect cell growth (human skin fibroblast cells). Herein, composite fibers with 6 wt% BG particle addition led to a higher density of adhered, spread, and proliferating cells.

In a parallel study, electrospun composite fibers composed of BG nanoparticles (composition: 76% SiO<sub>2</sub>-18% CaO-6% P<sub>2</sub>O<sub>5</sub>

(wt%), concentration: 5–40 wt%, size: 800 nm) incorporated in PVA-chitosan displayed a skin regeneration promotion effect (Figure 7A1-A8). In this regard, the implantation of such composite fibers in a rat full-thickness skin defect model and in a mice diabetic chronic wound model led to complete re-epithelialization and collagen alignment as a function of BG addition. This phenomenon originates from the capability of the BG nanoparticles for upregulating influential factors, including vascular endothelial growth factor and transforming growth factor- $\beta$ , and downregulating inflammatory cytokines such as tumor necrosis factor- $\alpha$  and interleukin 1 $\beta$ .<sup>[50]</sup>

Moreover, Saha et al.<sup>[109]</sup> evaluated the influence of silver-containing BG particles (composition: 1-2% B<sub>2</sub>O<sub>3</sub>-68-69% SiO<sub>2</sub>, 1 × 10<sup>-3</sup>% Ag<sub>2</sub>O-29-30% CaO (mol%), size: 200–900 nm) on the wound-healing capability of electrospun fibers based on polyvinyl-butyril (2:3). Here, the addition of BG particles led to improvement in skin fibroblast cell proliferation (24 h), confirming their wound-healing potential.

An innovative composite nanofiber was developed by combining cellulose acetate with 3 wt% BG nanoparticles in the investigation of Sharaf et al.<sup>[110]</sup> The electrospun nanofibers were identified as antimicrobial substrates against gram-negative and gram-positive bacteria. An in vivo study using a diabetic model of male Sprague Dawley rats (nearly 100–120 g) indicated that throughout the 10th day, the wound had already closed due to the incorporation of BG into the polymeric fiber composition. It was determined that on the first, fifth, tenth, and fifteenth day after treatment, the wound areas of the treated rats were 95.7 ± 1.8, 36.4 ± 3.2, 6.3 ± 1.5, and 0.8 ± 0.9, illustrating that composite fibers can be used in wound dressings to promote healing.

Zhang et al.<sup>[111]</sup> developed a micropatterned electrospun scaffold based on BG nanoparticles (concentration: 20 wt%, size: 50–100 nm)-containing PLA fibers to improve angiogenesis in diabetic wounds and to accelerate the healing process. CD31 and vascular endothelial growth factor expression as well as collagen deposition after 7 days were reported, indicating the angiogenic ability of the endothelial cell-cultured BG-containing fibers for the repair of chronic diabetic wounds.

In research conducted by Solanki et al.,<sup>[112]</sup> BG was modified using magnesium and cobalt to reduce calcium and phosphate content aiming at stimulating hypoxia to induce angiogenesis. The goal was the fabrication of BG (composition: 50% SiO<sub>2</sub>-24% Na<sub>2</sub>O-24% MgO-2% CoO (mol%), concentration: 30 wt%)-embedded PCL fibers for wound healing applications without formation of HA-like layers. The interaction of fibroblasts and BG containing medium stabilized the hypoxia-inducible factor-1 $\alpha$  showing an increase in angiogenesis-related protein production as well as higher expression of vascular endothelial growth factor.

Jana et al.<sup>[113]</sup> fabricated composite electrospun mats as wound dressings composed of fish (Rohu) skin-derived collagen and BG particles (concentration: 12–15 wt%) without and with dopants (3 and 5 wt% Cu and Co, respectively) to improve wound healing. Composite fibers provided a suitable environment for adhesion and proliferation of human dermal fibroblasts, as well as suitable blood compatibility against rabbit red blood cells. In vivo experiments with rabbits indicated continuous epidermis formation and wound maturity, as well as deposition of the ECM components collagen and elastin. Here, copper and cobalt ion doped

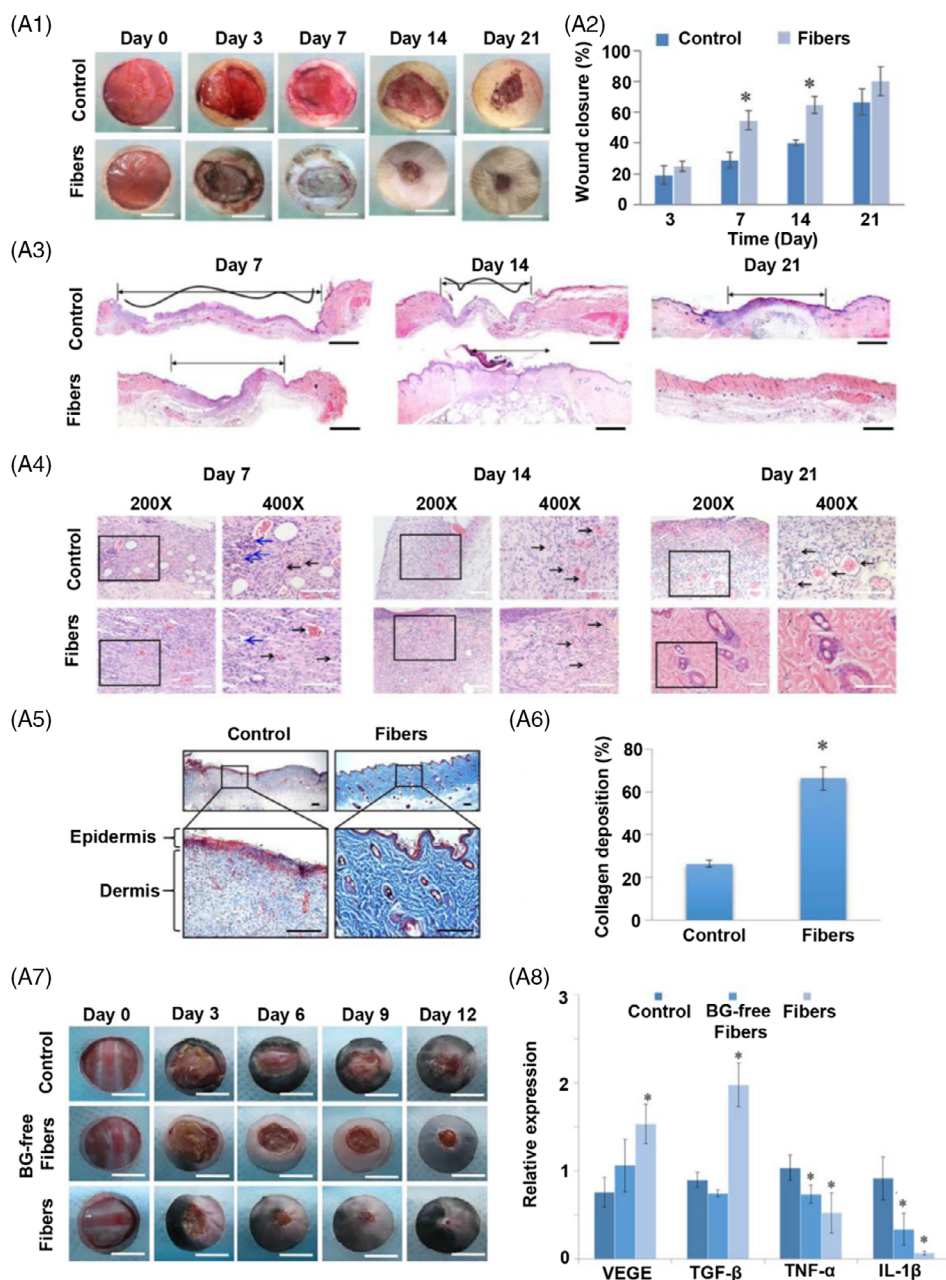


**Figure 7.** Performance of BG-containing PVA-chitosan fibers on rat full-thickness cutaneous wound healing. A1) optical image of full-thickness skin defects treated with the petrolatum gauze (Control) and BG-containing PVA-chitosan fibers after implantation (scale bar: 10 mm). A2) Wound closure level. A3) H&E staining for the gross wound (Scale bar: 2 mm). A4) H&E staining to evaluate histologic changes during healing (Scale bar: 100  $\mu$ m). A5,A6) quantified result of Masson's trichrome staining for collagen formation after 21 days treatment (Scale bar: 200  $\mu$ m, \* $p < 0.05$  (versus Control)). BG-containing PVA-chitosan fibers accelerated chronic wound healing on a diabetic mice full-thickness skin traumatic model. A7) Optical image of wound closure with petrolatum gauze (Control), BG-free fibers, and BG-containing PVA-chitosan fibers (Scale bar: 5 mm.) A8) Related gene expression of growth factors (VEGF: vascular endothelial growth factor, TGF- $\beta$ : transforming growth factor- $\beta$ ) and inflammatory cytokines (TNF- $\alpha$ : tumor necrosis factor- $\alpha$ , IL-1 $\beta$ : Interleukin-1 $\beta$ ) in diabetic wounds. Reproduced with permission.<sup>[50]</sup> Copyright 2019, Elsevier

BG-containing fibers showed a higher density of blood vessels, confirming neo-vascularization at the beginning of the healing process and remodeling of cutaneous structural components. **Table 5** presents a summary of investigations on BG-containing electrospun composite fibers in hard and soft TE applications.

### 3. Discussion and Outlook

Although various technologies have been applied to fabricate scaffolds for TE, a growing interest has emerged in the development of fibrous scaffolds by electrospinning due to the achieved

**Table 5.** Summary of reviewed studies on BG-containing electrospun composite fibers in hard and soft TE..

Composition	BG features	Solvent	Doping ion	Application	Properties	References
POC-BG	Composition: 70SiO <sub>2</sub> -25CaO-5P <sub>2</sub> O <sub>5</sub>  Concentration: 5, 10, and 15 % w/w	Ethanol	–	Bone TE	-Stimulating cell growth, -Increasing ALP activity -Improving cellular mineralization -Supporting osteogenic differentiation	[49]
PLLA-BG	Composition: 89% SiO <sub>2</sub> -8% CaO-3% P <sub>2</sub> O <sub>5</sub> (wt%)	Chloroform	–	Bone TE	-Improving bone marrow mesenchymal stem cells attachment, growth, proliferation -Calcium phosphate deposition after 14 days -Expression of ALP, osteocalcin, osteopontin, collagen I, and RUNX2 à osteogenic activity	[86]
PLA-BG	Composition: 70SiO <sub>2</sub> -25CaO-5P <sub>2</sub> O <sub>5</sub>  Concentration: up to 10 wt%	Chloroform	–	Hard TE	-Improving osteoblastic cells adhesion and growth -In vitro HA precipitation	[84]
PHB-PCL-BG	Composition: 58S, Concentration: 0–16.7 wt%	Chloroform-N,N-dimethyl formamide	–	Bone TE	-Suitable adhesion and viability of MG-63 cell -Increasing expression of ALP -Higher mineral calcium nodule content	[85]
PVA-SF-BG	Composition: 60% SiO <sub>2</sub> -36% CaO-4% P <sub>2</sub> O <sub>5</sub>  Size: <100 nm	DI-water	–	Bone TE	-Stiffness -Hydrophilicity Superior bioactivity -Excellent mesenchymal stem cell attachment, spreading, proliferation -Osteogenic differentiation. -Formation of bone-like nodules—increasing ALP activity and osteocalcin expression -Biom mineralization	[88]
PCL-BG	Composition: 5% SiO <sub>2</sub> ; 24.5% CaO; 24.5% Na <sub>2</sub> O and 6% P <sub>2</sub> O <sub>5</sub>  Concentration: 10 wt%)	Acetone	–	Bone TE	-Nucleation of the apatite layer on the fibers -Nodules mineralization after culturing the MSCs in nonosteogenic medium -Osteogenic differentiation of MSCs -In vivo formation of trabecular bone	[87]
Collagen-hollow BG	Composition: 46.13% SiO <sub>2</sub> -24.35% Na <sub>2</sub> O-26.91% CaO-2.6% P <sub>2</sub> O <sub>5</sub> (mol%)  Size: 240 nm	Ethanol:water (1:1)	–	Bone TE	-Outstanding hydrophilicity -Bioactivity -Superior mechanical properties -Improved cell adhesion and proliferation as well as cell orientation -Enhancing osteogenic performance -ALP activity -Vascularization	[99]
Collagen-chitosan-BG	Composition: Si/Ca/P = 80:15:5 mole ratio Hexafluoroisopropanol-trifluoroacetic acid		–	Periodontal TE	-Increasing human periodontal ligament cells viability -Osteogenic gene expression -Implantation of constructs in dog class II furcation defect model à promote in bone formation and mineralization.	[89]
Gelatin-BG	Composition: 70% SiO <sub>2</sub> -25% CaO-5% P <sub>2</sub> O <sub>5</sub> (mol%)  Concentration: ≈3 μm	Acetic acid	–	Bone TE	-Formation of multicellular layers -Improving ALP activity	[91]

**Table 5.** Continued.

Composition	BG features	Solvent	Doping ion	Application	Properties	References
Collagen-BG	Composition: Si/Ca/P = 80:15:5 mole ratio	Hexafluoroisopropanol	–	Skin TE	-Increasing cell adhesion -Increasing secretion of collagen type I and vascular endothelial growth factor	[92]
SF-BG	Composition: 70S	DI-water	–	Osteochondral TE	-Improving cellular performance -Increasing ALP activity	[93]
Poly hydroxyl butyrate-chitosan-BG	Composition: 45SS  Size: 35–55 nm	Trifluoro acetic acid	–	Dentin TE	-Nontoxicity -Appropriate cell adhesion and proliferation -Positive CD90 and CD146 markers -Differentiation of human exfoliated deciduous teeth stem cells -A sixfold enhancement in dentin sialophosphoprotein expression and collagen type I -A twofold enhancement in ALP activity	[94,95]
PCL-BG	Composition: 58S  Size: 38 $\mu$ m  Concentration: 5 wt%	Methanol:chloroform	–	Bone TE	- Hydrophilicity -HA formation after a 21 day soaking in the SBF solution -Dental pulp stem cells adhesion and proliferation -Matrix mineralization -Surface roughness $\rightarrow$ cell anchorage site	[96]
PCL-BG	Composition: F18	Dichloromethane: dimethylformamide (90:10)	–	Bone TE	-Increasing tensile strength -Increasing ALP activity after a 14 day incubation of MG-63 cells in fiber-containing media -Outstanding osteogenic performance	[97]
Polyamide 6-BG	Size: 2–30 $\mu$ m	Formic acid: acetic acid (4:1)	–	Bone TE	-High proliferation, viability and spreading of MC3T3 cells—osteogenic differentiation -Accelerated expression of late osteoblast marker genes -Large degree of apatite formation during incubation in physiological solution	[100]
PCL-BG	Composition: 85% SiO <sub>2</sub> , 12% CaO and 3%MgO synthesized by the Stober process  Concentration: 5, 10, 15 wt%  Size: 300 nm	Glacial acetic acid	–	Guided bone regeneration in dental implantology	-Barrier membranes for guided bone regeneration -Enhanced wettability in 5 wt% BG addition -High biomineralization in 10 and 15 wt% BG addition	[101]
PCL-BG	Composition: 60% SiO <sub>2</sub> , 36% CaO, and 4% P <sub>2</sub> O <sub>5</sub> (mol%), Concentration: 20 (wt%)  Size: BGNFs: 450 nm BGP: 4 $\mu$ m	Tetrahydroforane	–	Bone TE	-BGNFs enhanced the stiffness of the composite. -BGNF-containing scaffolds demonstrated better biocompatibility over BGP-containing ones. -Improvement of bioactivity in a physiological environment after using BGNFs -In vivo bone regeneration in calvarial defects of Sprague-Dawley albino rats	[102]
Chitosan-poly ethylene oxide-BG	Composition: Standard 45SS  Size: 10–20 $\mu$ m	Acetic acid-water	–	Orthopedic applications	-Improved biomineralization	[46]



**Table 5.** Continued.

Composition	BG features	Solvent	Doping ion	Application	Properties	References
					-Expression of osteocalcin and osteopontin after SaOS-2 human osteosarcoma cell line culture -Stimulate osteoblast to secrete bone ECM	
Zein-BG	Concentration: 15 wt% Composition: 45S5 Size: 4 $\mu$ m Concentration: 2, 4, and 9 wt%	Acetic acid	Copper	TE	-Reducing Young's modulus and ultimate tensile strength as a function of BG addition -Antibacterial activity copper-containing BGs -Osteogenic and angiogenic ability -Increasing the number of MG-63 and C2C12 cells	[98]
PCL-collagen-BG	Composition: 60% SiO <sub>2</sub> -36% CaO-4% P <sub>2</sub> O <sub>5</sub> (mol%) Size: 100 nm	Ethanol:water (7:3)	–	Wound healing	-Improvement in expression of CD31, vascular endothelial growth factor, and hypoxia-inducible factor 1- $\alpha$ expression -Collagen-type III deposition -Angiogenesis	[107]
PCL-BG	Composition: 77S Size: 300–710 $\mu$ m Concentration: 0–8 wt%	Dichloromethane: dimethyl formamide (7:3)	–	Skin TE	-Reduction in fiber diameter as a function of BG addition -Composite fibers with 6 wt% BG indicated the higher density of the adhered, spread, and proliferated cell	[108]
PVA-chitosan-BG	Composition: 76SiO <sub>2</sub> -18CaO-6P <sub>2</sub> O <sub>5</sub> Size: 800 nm Concentration: 5–40 wt%	Trifluoroacetic acid: dichloromethane (7:3, v/v)	–	Skin TE	-Implantation of composite fibers in rat full-thickness skin defects model and mice diabetic chronic wound model à complete re-epithelialization and collagen alignment as a function of BG addition -Upregulating vascular endothelial growth factor and transforming growth factor- $\beta$ -Downregulating inflammatory cytokines such as tumor necrosis factor- $\alpha$ and interleukin 1 $\beta$	[50]
Polyvinyl butyral-BG	Composition: 1–2% B <sub>2</sub> O <sub>3</sub> -68–69% SiO <sub>2</sub> -1 $\times$ 10 – 3% Ag <sub>2</sub> O-29–30% CaO (mol%) Size: 200–900 nm	Ethanol:water (7:3)	–	Wound healing	-Improvement in skin fibroblast cells proliferation (24 h)	[109]
Cellulose acetate-BG	Concentration: 3 wt%	N,N-dimethyl acetamide-acetone	–	Wound healing	-Antimicrobial performance against gram-negative and gram-positive bacteria -Wound closure during 10 days in rat model	[110]
PLA-BG	Size: 50–100 nm Concentration: 20 wt%	–	–	Wound healing	-Improving angiogenesis in diabetic wounds -Accelerating the healing process. -Expression of CD31 and vascular endothelial growth factors -Collagen deposition after 7 days -Angiogenesis	[111]
PCL-BG	Composition: 50% SiO <sub>2</sub> -24% Na <sub>2</sub> O-24% MgO-2% CoO (mol%) Concentration: 30 wt%	Chloroform	Magnesium and cobalt	Wound healing	-Stabilizing hypoxia-inducible factor-1 $\alpha$ -Increasing angiogenesis-related protein production -Higher expression of vascular endothelial growth factor	[112]
Fish (Rohu) skin-derived collagen-BG	Concentration: 12–15 wt%	1,1,1,3,3,3-hexafluoro-2-propanol	Copper and cobalt	Wound dressing	-Adhesion and proliferation of human dermal fibroblasts	[113]

**Table 5.** Continued.

Composition	BG features	Solvent	Doping ion	Application	Properties	References
					-Blood compatibility -In vivo epidermis formation and wound maturity -Deposition of ECM component, collagen, and elastin -Higher density of blood vessels, confirming neo-vascularization as function of copper and cobalt addition	
Collagen/Silk fibroin/BG	Composition: SiO <sub>2</sub> -CaO (crystalline) Size: 37 nm	Acetic acid + water	-	Bone TE	Improved bone growth performance in OVX rats' in vivo critical-sized bone defect. Increased blood vessel development, mineral deposition, and improved bone metabolism.	[134]
Co-axial fibers based on mesoporous BG modified with insulin-like growth factor-1 (IGF-1) as core and silk fibroin (SF) - vascular endothelial growth factor (VEGF) as shell	SiO <sub>2</sub> -CaO-P <sub>2</sub> O <sub>5</sub> Exact composition not given, particle size not given	1,1,1,3,3,3-hexafluoro-2-propanol	-	Bone TE	Enhanced bone defect repair and accelerating angiogenesis	[135]
PCL-BG	5S5 BG	-	Zn	Bone TE	Osteogenesis proved by ALP activity and formation of mineralization nodules	[136]

high volume to surface area and the fibrous structure resembling the ECM architecture. Electrospinning is a powerful technology for manipulating the properties of materials down to the nanoscale, which is the same dimensional level of native ECM components, e.g., proteins. In this regard, it is essential that the interactions between cells and the fibrous matrix are such that the effectiveness of the regeneration process is maximized. To gain a better understanding of the cell-fibrous scaffold interaction, further research is required regarding the influence of nanofibers on cellular signaling mechanisms as well as biochemical pathways. Despite the advantages of electrospun composite fibers, there are a number of environmental concerns connected to solution electrospinning since it involves organic solvents. In this particular case, melt electrospinning allows for the avoidance of the use of potentially toxic organic solvents. It is pertinent to note that despite the advantages of melt electrospinning, the method has some limitations as a result of its low throughput, which led to the adoption of solution-based electrospinning as a convenient industrial technology. It is also crucial that a reliable quality control system be in place before the production process can be scaled up. Approaches such as nozzle-free industrial scale electrospinning instruments are being explored to improve the production throughput.<sup>[114]</sup> Another drawback of this method is that it restricts fabricating composite fibers based on electrosensitive polymers or biomolecules, which need to be processed by alternative fiber production approaches without the usage of electrical fields, such as the nozzle-free centrifugal spinning method. However, electrospun fibers provide a suitable architecture for cell adhesion, proliferation, differentiation, and vascularization. Embedding bioactive inorganic particles into the polymeric matrix is increasingly being investigated for TE applications due to the extra functionality provided by the filler. As reviewed in this paper, the biomimetic formation of HA-like layers induced by addition of BG fillers improves

for instance bone regeneration as well as wound healing. Incorporation and conjugation of BG particles (both micron sized and nanoscaled) in polymeric fibers have been explored, showing strong potential to control cell-scaffold interactions for supporting tissue regeneration. BGs are the bioactive materials of choice for combination with biopolymer fibers due to their bioactivity leading to improved cellular functions, including facilitating biomineralization, osteogenic differentiation, vascularization, and antibacterial effects. Additionally, the advantages of BG-containing fibers in comparison to other incorporated bioactive materials such as HA or  $\beta$ -TCP have been confirmed in several studies, observing better mineralization, cell adhesion, and proliferation, as well as cell differentiation and gene upregulation. Besides, the type and chemical composition of the used BG needs to be considered as an influential factor in the final performance of composite fibers. Here, the addition of silicate BGs such as 45S5 BG leads to carbonate HA precipitation, which has the highest similarity to physiological HA composition. However, the degradation of some silicate BGs increases the ionic by-products content and it could lead to potential toxic effects by changing the local pH. Accordingly, borate BGs or 13-93 BG compositions are preferred in some cases due to their controllable biodegradation rate. Nevertheless, the toxicity of the released boron in B<sub>2</sub>O<sub>3</sub>-rich BGs, especially in static culture, is a concern even though a reduced level of toxicity has been observed in animal models.<sup>[115,116]</sup> On the other hand, the antibacterial properties of boron make these glasses an appropriate option for controlling bacterial infection during tissue regeneration.<sup>[67]</sup> The other alternative can be phosphate BG-based fibers, which have shown controllable degradation rate compared with silicate BG-containing composites. Nonetheless, the risk of inflammation reactions during biodegradation provides restrictions in the biomedical applications of highly degradable BG-containing fibers. It is worthy to consider that the composite fibers

incorporating BG can exhibit a range of extra functionalities, including anti-inflammatory, immunomodulatory, antibacterial and antioxidant activities, through incorporation of dopant ions, which indicates a distinct advantage of composite fibers based on BG particles. In this article, we presented a comprehensive overview of BG-based composite fibers, including a detailed review of the processing parameters established in different studies to reach the required mechanical properties as well as appropriate cellular interactions. Electrospun BG-embedded composite fibers' physicochemical, mechanical, and in vitro properties were discussed as a function of different factors, especially the type of BG used. Both melt-derived and sol-gel derived BG particles have been used, leading to different outcomes given the different basic characteristics of the particles produced by both methods, as discussed in this review. Increasing fiber diameter as a function of BG addition and smaller pore sizes (when the fiber arrangement is the same) have been reported, which may restrict cell infiltration affecting cell ingrowth and vascularization, especially in thick bone defects. Other concerns regarding composite fibers include nanoparticle agglomeration in the polymer matrix and lack of specific interactions between the organic and inorganic phases. Although higher surface areas arise from the addition of nanoparticles, which can increase ion release rate and surface reactivity, as well as protein adsorption and cell responses, the agglomeration of particles might lead to undesirable nanoparticle dispersions, reduced mechanical strength of the fibers, and unfavorable cellular responses. In this regard, an alternative approach to generate bioactive fibers involves the direct electrospinning from a sol, or sol-gel hybrid, which does not require a separate glass particle addition to the polymer.<sup>[117]</sup> This method leads to the formation of BG-hybrid fibers with a uniform and homogenous structure. It is interesting to note that direct writing electrospinning, inspired by additive manufacturing, can be used in clinical applications to produce individualized three-dimensional matrices with distinct characteristics, while micrometer-scale fibers produced by this technique are not a good choice for nano-bioapplications. Nanofibers are particularly favorable in the context of tissue models, as well as for manipulating cell interactions at the nanoscale to facilitate tissue reconstruction. Therefore, understanding the mechanism behind different electrospinning techniques in order to be able to predict the final structure and properties of fibers in a more accurate manner is crucial. It can be anticipated that clinical and translational studies on electrospun BG-containing composite fibers for hard and soft tissues will lead to medical applications, especially for bone tissue regeneration and wound-healing, although such a translational goal remains a long way off. As is the case for all developing, novel biomaterials, translating concepts, and commercializing them face several challenges, including long-term immunogenicity, biocompatibility, as well as differences between in vivo results in animal models and in human patients. As a result of the multifunctionality and stratification of tissues, the repair process requires complex, hierarchical scaffolds. Hence, the combination of additive manufacturing and electrospinning provides 3D nanofibrous matrices that can help to fulfill the above-mentioned goal. Thus, BG-biopolymer composite electrospun fibers combined with 3D printing should be explored in future studies. Here, portable devices, as already available,<sup>[118]</sup> are important to facilitate the translation of

electrospinning-based products. The authors hope that this review will serve as a basic source of information about the state-of-the-art of research in this expanding field, and will promote further interest on electrospun BG-containing composite fibers toward translational biomedical applications.

## Acknowledgements

This work was supported by Alexander von Humboldt Foundation (fellowship to FG).

Open Access funding enabled and organized by Projekt DEAL.

## Conflict of Interest

The authors declare no conflict of interest.

## Author Contributions

F.G.: Conceptualization, methodology, validation, investigation, data curation, visualization, writing—original draft—review and editing. T.R.: Investigation, methodology, writing—original draft. L.L.: Validation, investigation, writing—review and editing. D.W.S.: Validation, investigation, supervision, writing—review, and editing. A.R.B.: Conceptualization, writing—review and editing, supervision, project administration, funding acquisition. J.A.R.: Conceptualization, methodology, validation, investigation, data curation, writing—review and editing.

## Keywords

bioactive glass, composites, electrospinning, fibers, tissue engineering

Received: July 28, 2022

Revised: December 10, 2022

Published online: January 18, 2023

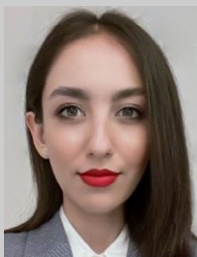
- [1] M. Rahmati, D. K. Mills, A. M. Urbanska, M. R. Saeb, J. R. Venugopal, S. Ramakrishna, M. Mozafari, *Prog. Mater. Sci.* **2021**, *117*, 100721.
- [2] T. Abudula, K. Gauthaman, A. Mostafavi, A. Alshahrie, N. Salah, P. Morganti, A. Chianese, A. Tamayol, A. Memic, *Sci. Rep.* **2020**, *10*, 20428.
- [3] Q. Cheng, B. L.-P. Lee, K. Komvopoulos, S. Li, *Biomacromolecules* **2013**, *14*, 1349.
- [4] J. Nam, Y. Huang, S. Agarwal, J. Lannutti, *Tissue Eng.* **2007**, *13*, 2249.
- [5] Y. Ding, W. Li, F. Zhang, Z. Liu, N. Zanjanzadeh Ezazi, D. Liu, H. A. Santos, *Adv. Funct. Mater.* **2019**, *29*, 1802852.
- [6] D. W. Schubert, *Macromol. Theory Simul.* **2019**, *28*, 1900006.
- [7] H.-Y. Mi, M. R. Salick, X. Jing, W. C. Crone, X.-F. Peng, L.-S. Turng, *J. Biomed. Mater. Res. Part A* **2015**, *103*, 593.
- [8] H. Hasmad, M. R. Yusof, Z. R. Mohd Razi, R. B. Hj Idrus, S. R. Chowdhury, *Tissue Eng. Part C Methods* **2018**, *24*, 368.
- [9] N. L. Nerurkar, B. M. Baker, S. Sen, E. E. Wible, D. M. Elliott, R. L. Mauck, *Nat. Mater.* **2009**, *8*, 986.
- [10] T. Chae, H. Yang, H. Moon, T. Troczynski, F. K. Ko, *ACS Appl. Bio Mater.* **2020**, *3*, 6746.
- [11] F. Ghorbani, B. Ghalandari, A. L. Khan, D. Li, A. Zamanian, B. Yu, *Biotechnol. Prog.* **2020**, *36*, e3043.

- [12] L. Zhu, S. Jia, T. Liu, L. Yan, D. Huang, Z. Wang, S. Chen, Z. Zhang, W. Zeng, Y. Zhang, H. Yang, D. Hao, *Adv. Funct. Mater.* **2020**, *30*, 2002610.
- [13] D. Grafahrend, K.-H. Heffels, M. V. Beer, P. Gasteier, M. Möller, G. Boehm, P. D. Dalton, J. Groll, *Nat. Mater.* **2011**, *10*, 67.
- [14] S.-J. Seo, C. Mahapatra, R. K. Singh, J. C. Knowles, H.-W. Kim, *J. Tissue Eng.* **2014**, *5*, 204173141454185.
- [15] X. Gao, S. Han, R. Zhang, G. Liu, J. Wu, *J. Mater. Chem. B* **2019**, *7*, 7075.
- [16] M. Li, X. Gao, X. Wang, S. Chen, J. Yu, *ACS Appl. Nano Mater.* **2021**, *4*, 2952.
- [17] M. Yu, Y. Du, Y. Han, B. Lei, *Adv. Funct. Mater.* **2020**, *30*, 1906013.
- [18] M. R. El-Aassar, O. M. Ibrahim, Z. H. Al-Qanzi, *Polymers (Basel)* **2021**, *13*, 3734.
- [19] L. Gao, Y. Zhou, J. Peng, C. Xu, Q. Xu, M. Xing, J. Chang, *NPG Asia Mater.* **2019**, *11*, 66.
- [20] P. Khoshakhlagh, S. M. Rabiee, G. Kiaee, P. Heidari, A. K. Miri, R. Moradi, F. Moztaizadeh, R. Ravarian, *Carbohydr. Polym.* **2017**, *157*, 1261.
- [21] Q. Ye, Y. Zhang, K. Dai, X. Chen, H. M. Read, L. Zeng, F. Hang, *J. Mater. Sci. Mater. Med.* **2020**, *31*, 77.
- [22] M. N. Rahaman, D. E. Day, B. Sonny Bal, Q. Fu, S. B. Jung, L. F. Bonewald, A. P. Tomsia, *Acta Biomater.* **2011**, *7*, 2355.
- [23] F. Ghorbani, B. Ghalandari, M. Sahranavard, A. Zamanian, M. N. Collins, *Mater. Sci. Eng. C* **2021**, *130*, 112434.
- [24] S.-M. Mousavi, Z. M. Nejad, S. A. Hashemi, M. Salari, A. Gholami, S. Ramakrishna, W.-H. Chiang, C. W. Lai, *Membranes (Basel)* **2021**, *11*, 702.
- [25] V. A. Revkova, K. V. Sidoruk, V. A. Kalsin, P. A. Melnikov, M. A. Konoplyannikov, S. Kotova, A. A. Frolova, S. A. Rodionov, M. M. Smorchkov, A. V. Kovalev, A. V. Troitskiy, P. S. Timashev, V. P. Chekhonin, V. G. Bogush, V. P. Baklaushev, *ACS Omega* **2021**, *6*, 15264.
- [26] L. D. Soule, N. Pajares Chomorro, K. Chuong, N. Mellott, N. Hammer, K. D. Hankenson, X. Chatzistavrou, *ACS Biomater. Sci. Eng.* **2020**, *6*, 5549.
- [27] M. S. Araujo, A. C. Silva, B. Cabal, J. F. Bartolomé, S. Mello-Castanho, *J. Mater. Res. Technol.* **2021**, *13*, 154.
- [28] H. Shin, S. Jo, A. G. Mikos, *Biomaterials* **2003**, *24*, 4353.
- [29] M. P. Lutolf, J. A. Hubbell, *Nat. Biotechnol.* **2005**, *23*, 47.
- [30] G. Jell, M. M. Stevens, *J. Mater. Sci. Mater. Med.* **2006**, *17*, 997.
- [31] J. Kettleach, D. Kaigler, Z. Wang, P. Krebsbach, D. Mooney, *Biomaterials* **2006**, *27*, 3249.
- [32] L. L. Hench, *Biomed. Glasses* **2015**, *1*, 1.
- [33] K. Zhang, B. Chai, H. Ji, L. Chen, Y. Ma, L. Zhu, J. Xu, Y. Wu, Y. Lan, H. Li, Z. Feng, J. Xiao, H. Zhang, K. Xu, *Lab. Invest.* **2022**, *102*, 90.
- [34] S. Homaeigohar, M. Li, A. R. Boccaccini, *Burn. Trauma* **2022**, *10*, <https://doi.org/10.1093/burnst/tkac038>.
- [35] K. T. Shalumon, S. Sowmya, D. Sathish, K. P. Chennazhi, S. V. Nair, R. Jayakumar, *J. Biomed. Nanotechnol.* **2013**, *9*, 430.
- [36] A. M. Deliormanli, R. Konyali, *J. Aust. Ceram. Soc.* **2019**, *55*, 247.
- [37] J. Ródenas-Rochina, J. L. G. Ribelles, M. Lebourg, *J. Mater. Sci. Mater. Med.* **2013**, *24*, 1293.
- [38] S. Haimi, N. Suuriniemi, A.-M. Haaparanta, V. Ellä, B. Lindroos, H. Huhtala, S. Rätty, H. Kuokkanen, G. K. Sándor, M. Kellomäki, S. Miettinen, R. Suuronen, *Tissue Eng. Part A* **2009**, *15*, 1473.
- [39] Y. Goh, M. Akram, A. Alshemary, R. Hussain, *Appl. Surf. Sci.* **2016**, *387*, 1.
- [40] V. Sunandhakumari, A. Vidhyadharan, A. Alim, D. Kumar, J. Ravindran, A. Krishna, M. Prasad, *Bioengineering* **2018**, *5*, 54.
- [41] D. Moura, M. T. Souza, L. Liverani, G. Rella, G. M. Luz, J. F. Mano, A. R. Boccaccini, *Mater. Sci. Eng., C* **2017**, *76*, 224.
- [42] R. Sergi, V. Cannillo, A. R. Boccaccini, L. Liverani, *Materials (Basel)* **2020**, *13*, 5651.
- [43] K. Schuhladden, S. N. V. Raghu, L. Liverani, Z. Neščáková, A. R. Boccaccini, *J. Biomed. Mater. Res. Part B Appl. Biomater.* **2021**, *109*, 180.
- [44] L. Liverani, J. Lacina, J. A. Roether, E. Boccardi, M. S. Killian, P. Schmuki, D. W. Schubert, A. R. Boccaccini, *Bioact. Mater.* **2018**, *3*, 55.
- [45] A. Saberi, M. Rafienia, E. Poorazizi, *Nanomedicine* **2017**, *4*, 152.
- [46] F. Boschetto, H. Ngoc Doan, P. Phong Vo, M. Zanocco, W. Zhu, W. Sakai, T. Adachi, E. Ohgitani, N. Tsutsumi, O. Mazda, K. Kinashi, E. Marin, G. Pezzotti, *Appl. Sci.* **2020**, *10*, 2360.
- [47] F. Serio, M. Miola, E. Vernè, D. Pisignano, A. Boccaccini, L. Liverani, *Nanomaterials* **2019**, *9*, 182.
- [48] M. Luginina, K. Schuhladden, R. Orrú, G. Cao, A. R. Boccaccini, L. Liverani, *Nanomaterials* **2020**, *10*, 978.
- [49] H. Lian, Z. Meng, *Mater. Sci. Eng., C* **2018**, *84*, 123.
- [50] Q. Chen, J. Wu, Y. Liu, Y. Li, C. Zhang, W. Qi, K. W. K. Yeung, T. M. Wong, X. Zhao, H. Pan, *Mater. Sci. Eng., C* **2019**, *105*, 110083.
- [51] R. Konyali, A. M. Deliormanli, *J. Thermoplast. Compos. Mater.* **2019**, *32*, 690.
- [52] L. Liverani, A. Liguori, P. Zezza, C. Gualandi, M. Toselli, A. R. Boccaccini, M. L. Focarete, *Bioact. Mater.* **2022**, *11*, 230.
- [53] R. Odermatt, M. Par, D. Mohn, D. B. Wiedemeier, T. Attin, T. T. Tauböck, *J. Clin. Med.* **2020**, *9*, 772.
- [54] S. Nazarneshad, F. Baines, H.-W. Kim, T. J. Webster, S. Kargozar, *Nanomaterials* **2020**, *10*, 1609.
- [55] D. Abebayehu, A. J. Spence, M. J. McClure, T. T. Haque, K. O. Rivera, J. J. Ryan, *J. Biomed. Mater. Res. Part A* **2019**, *107*, 884.
- [56] H. Elkhoul, W. Mamdouh, D. I. El-Korashy, *J. Mater. Sci. Mater. Med.* **2021**, *32*, 111.
- [57] D. A. Canales, F. Reyes, M. Saavedra, L. Peponi, A. Leonés, H. Palza, A. R. Boccaccini, A. Grünewald, P. A. Zapata, *Int. J. Biol. Macromol.* **2022**, *210*, 324.
- [58] P. S. Kandelousi, S. M. Rabiee, M. Jahanshahi, F. Nasiri, *J. Bioact. Compat. Polym.* **2019**, *34*, 97.
- [59] H. Nosrati, M. Banitalebi-Dhkordi, M. Khodaei, E. Sharifi, S. Asadpour, K. Mansouri, M. Soleimannejad, *J. Shahrekord Univ. Med. Sci.* **2022**, *24*, 1.
- [60] R. Iron, M. Mehdkhani, E. Naghashzargar, S. Karbasi, D. Semnani, *Mater. Technol.* **2019**, *34*, 540.
- [61] C. Wang, H. Chen, X. Zhu, Z. Xiao, K. Zhang, X. Zhang, *Mater. Sci. Eng., C* **2017**, *70*, 1192.
- [62] M. Erol-Taygun, I. Unalan, M. I. B. Idris, J. F. Mano, A. R. Boccaccini, *Adv. Eng. Mater.* **2019**, *21*, 1900287.
- [63] B. N. Singh, K. Pramanik, *J. Biomater. Sci. Polym. Ed.* **2018**, *29*, 2011.
- [64] E. Tamjid, R. Bagheri, M. Vossoughi, A. Simchi, *Mater. Sci. Eng., C* **2011**, *31*, 1526.
- [65] M. R. Foroughi, S. Karbasi, M. Khoroushi, A. A. Khademi, *J. Porous Mater.* **2017**, *24*, 1447.
- [66] A. Hoppe, V. Mouriño, A. R. Boccaccini, *Biomater. Sci.* **2013**, *1*, 254.
- [67] E. Munukka, O. Leppäranta, M. Korkeamäki, M. Vaahtio, T. Peltola, D. Zhang, L. Hupa, H. Ylänen, J. I. Salonen, M. K. Viljanen, E. Eerola, *J. Mater. Sci. Mater. Med.* **2008**, *19*, 27.
- [68] K. R. Raghupathi, R. T. Koodali, A. C. Manna, *Langmuir* **2011**, *27*, 4020.
- [69] E. Alpaslan, B. M. Geilich, H. Yazici, T. J. Webster, *Sci. Rep.* **2017**, *7*, 45859.
- [70] A. Bari, N. Bloise, S. Fiorilli, G. Novajra, M. Vallet-Regí, G. Bruni, A. Torres-Pardo, J. M. González-Calbet, L. Visai, C. Vitale-Brovarene, *Acta Biomater.* **2017**, *55*, 493.
- [71] F. Ciraldo, L. Liverani, L. Gritsch, W. Goldmann, A. Boccaccini, *Materials (Basel)* **2018**, *11*, 692.



- [72] S. Naseri, W. C. Lepry, S. N. Nazhat, *J. Mater. Chem. B* **2017**, 5, 6167.
- [73] D. S. Brauer, *Angew. Chem. Int. Ed.* **2015**, 54, 4160.
- [74] I. Rajzer, M. Dziadek, A. Kurowska, K. Cholewa-Kowalska, M. Ziabka, E. Menaszek, T. E. L. Douglas, *J. Mater. Sci. Mater. Med.* **2019**, 30, 80.
- [75] Z. Neščáková, H. Kaňková, D. Galusková, D. Galusek, A. R. Boccaccini, L. Liverani, *Int. J. Appl. Glass Sci.* **2021**, 12, 588.
- [76] A. Saatchi, A. R. Arani, A. Moghanian, M. Mozafari, *Ceram. Int.* **2021**, 47, 260.
- [77] B. Malekahmadi, V. Esfahanian, F. Ejeian, M. E. Dastgardi, M. Agheb, F. Kaveian, M. Rafenia, M. H. Nasr-Esfahani, *Biomimetics* **2022**, 7, 19.
- [78] A. Akturk, M. Erol-Taygun, G. Goller, S. Küçükbayrak, *Chem. Pap.* **2021**, 75, 5929.
- [79] S. Chen, D. Galusková, H. Kaňková, K. Zheng, M. Michálek, L. Liverani, D. Galusek, A. R. Boccaccini, *Materials (Basel)* **2020**, 13, 4010.
- [80] A. M. Deliormanli, B. Rahman, S. Oguzlar, K. Ertekin, *J. Mater. Sci.* **2021**, 56, 14487.
- [81] K. Duan, Z. Ling, M. Sun, W. Zhi, Y. Zhang, S. Han, J. Xu, H. Wang, J. Li, *J. Appl. Polym. Sci.* **2022**, 139, 51746.
- [82] J. S. Fernandes, P. Gentile, M. Martins, N. M. Neves, C. Miller, A. Crawford, R. A. Pires, P. Hatton, R. L. Reis, *Acta Biomater.* **2016**, 44, 168.
- [83] M. Lotfi, M. Nejib, M. Naceur, *Advances in Biomaterials Science and Biomedical Applications*, IntechOpen, London, United Kingdom **2013**.
- [84] K.-T. Noh, H.-Y. Lee, U.-S. Shin, H.-W. Kim, *Mater. Lett.* **2010**, 64, 802.
- [85] Y. Ding, W. Li, T. Müller, D. W. Schubert, A. R. Boccaccini, Q. Yao, J. A. Roether, *ACS Appl. Mater. Interfaces* **2016**, 8, 17098.
- [86] M. Shamsi, M. Karimi, M. Ghollasi, N. Nezafati, M. Shahrivand, M. Kamali, A. Salimi, *Mater. Sci. Eng., C* **2017**, 78, 114.
- [87] G. F. da Fonseca, S. de O. M. Avelino, D. de C. R. Mello, R. F. do Prado, T. M. B. Campos, L. M. R. de Vasconcellos, E. de Sousa Trichês, A. L. S. Borges, *J. Mater. Sci. Mater. Med.* **2020**, 31, 41.
- [88] B. N. Singh, K. Pramanik, *Biofabrication* **2017**, 9, 015028.
- [89] T. Zhou, X. Liu, B. Sui, C. Liu, X. Mo, J. Sun, *Biomed. Mater.* **2017**, 12, 055004.
- [90] M. S. El-Okaily, A. M. EL-Rafei, M. Basha, N. T. Abdel Ghani, M. M. H. El-Sayed, A. Bhaumik, A. A. Mostafa, *Int. J. Biol. Macromol.* **2021**, 182, 1582.
- [91] C. Gao, Q. Gao, Y. Li, M. N. Rahaman, A. Teramoto, K. Abe, *J. Appl. Polym. Sci.* **2013**, 127, 2588.
- [92] T. Zhou, B. Sui, X. Mo, J. Sun, *Int. J. Nanomed.* **2017**, 12, 3495.
- [93] J. C. M, P. J. T. Reardon, R. Konwarh, J. C. Knowles, B. B. Mandal, *ACS Appl. Mater. Interfaces* **2017**, 9, 8000.
- [94] B. Hashemi-Beni, M. Khoroushi, M. R. Foroughi, S. Karbasi, A. A. Khademi, *Dent. Res. J. (Isfahan)* **2018**, 15, 136.
- [95] M. Khoroushi, M. R. Foroughi, S. Karbasi, B. Hashemibeni, A. A. Khademi, *Mater. Sci. Eng., C* **2018**, 89, 128.
- [96] S. Labbaf, A. B. Houreh, M. Rahimi, H.-K. Ting, J. Jones, M. Nasr-Esfahani, *Biomed. Glass* **2018**, 4, 123.
- [97] L. Hidalgo Pitaluga, M. Trevelin Souza, E. Dutra Zanotto, M. Santocildes Romero, P. Hatton, *Materials (Basel)* **2018**, 11, 400.
- [98] C. E. Mariotti, L. Ramos-Rivera, B. Conti, A. R. Boccaccini, *Macromol. Biosci.* **2020**, 20, 2000059.
- [99] D. Dhinasekaran, S. Vimalraj, A. R. Rajendran, S. Saravanan, B. Purushothaman, B. Subramaniam, *Mater. Sci. Eng., C* **2021**, 126, 111856.
- [100] A. Abdal-hay, F. A. Sheikh, A. N. Shmroukh, H. M. Mousa, Y.-K. Kim, S. Ivanovski, *Mater. Des.* **2021**, 210, 110094.
- [101] Z. Tabia, S. Akhtach, M. Bricha, K. El Mabrouk, *Eur. Polym. J.* **2021**, 161, 110841.
- [102] J. H. Jo, E. J. Lee, D. S. Shin, H. E. Kim, H. W. Kim, Y. H. Koh, J. H. Jang, *J. Biomed. Mater. Res. Part B Appl. Biomater.* **2009**, 91, 213.
- [103] Hamed Nosrati, Z. Alizadeh, M. Khodaei, M. Banitalebi-Dehkordi, *Cell Tissue Biol.* **2021**, 15, 409.
- [104] H. Yu, J. Peng, Y. Xu, J. Chang, H. Li, *ACS Appl. Mater. Interfaces* **2016**, 8, 703.
- [105] Y. Jiang, Y. Han, J. Wang, F. Lv, Z. Yi, Q. Ke, H. Xu, *ACS Appl. Bio Mater.* **2019**, 2, 787.
- [106] S.-H. Jeong, D.-Y. Shin, I.-K. Kang, E.-H. Song, Y.-J. Seong, J.-U. Park, H.-E. Kim, *ACS Biomater. Sci. Eng.* **2018**, 4, 2380.
- [107] W. Gao, W. Jin, Y. Li, L. Wan, C. Wang, C. Lin, X. Chen, B. Lei, C. Mao, *J. Mater. Chem. B* **2017**, 5, 7285.
- [108] Z. Lin, W. Gao, L. Ma, H. Xia, W. Xie, Y. Zhang, X. Chen, *J. Bioact. Compat. Polym.* **2018**, 33, 195.
- [109] S. Saha, A. Bhattacharjee, S. H. Rahaman, S. Ray, M. K. Marei, H. Jain, J. Chakraborty, *Int. J. Appl. Glass Sci.* **2020**, 11, 320.
- [110] S. S. Sharaf, A. M. El-Shafei, R. Refaie, A. A. Gibriel, R. Abdel-Sattar, *Cellulose* **2022**, 29, 4565.
- [111] P. Zhang, Y. Jiang, D. Liu, Y. Liu, Q. Ke, H. Xu, *Nanomedicine* **2020**, 15, 2241.
- [112] A. K. Solanki, F. V. Lali, H. Autefage, S. Agarwal, A. Nommeots-Nomm, A. D. Metcalfe, M. M. Stevens, J. R. Jones, *Biomater. Res.* **2021**, 25, <https://doi.org/10.1186/s40824-020-00202-6>.
- [113] S. Jana, P. Datta, H. Das, P. R. Ghosh, B. Kundu, S. K. Nandi, *ACS Biomater. Sci. Eng.* **2022**, 8, 734.
- [114] J. J. Rogalski, C. W. M. Bastiaansen, T. Peijs, *Nanocomposites* **2017**, 3, 97.
- [115] S. B. Jung, D. E. Day, R. F. Brown, L. F. Bonewald, *Ceramic Engineering and Science Proceedings*, Vol. 3, no. 6, Wiley-Blackwell, January **2013**, pp. 65–74.
- [116] R. F. Brown, M. N. Rahaman, A. B. Dwilewicz, W. Huang, D. E. Day, Y. Li, B. S. Bal, *J. Biomed. Mater. Res., Part A* **2009**, 88A, 392.
- [117] B. A. Allo, A. S. Rizkalla, K. Mequanint, *Langmuir* **2010**, 26, 18340.
- [118] J. Haik, R. Kornhaber, B. Blal, M. Harats, *Adv. Wound Care* **2017**, 6, 116.
- [119] N. Silvestry-Rodriguez, E. E. Sicairos-Ruelas, C. P. Gerba, K. R. Bright, *Rev. Environ. Contam. Toxicol.* **2007**, 191, 23.
- [120] S.-H. Luo, W. Xiao, X.-J. Wei, W.-T. Jia, C.-Q. Zhang, W.-H. Huang, D.-X. Jin, M. N. Rahaman, D. E. Day, *J. Biomed. Mater. Res. Part B Appl. Biomater.* **2010**, 95B, 441.
- [121] A. M. El-Kady, A. F. Ali, R. A. Rizk, M. M. Ahmed, *Ceram. Int.* **2012**, 38, 177.
- [122] A. J. Salinas, S. Shruti, G. Malavasi, L. Menabue, M. Vallet-Regí, *Acta Biomater.* **2011**, 7, 3452.
- [123] V. Aina, G. Malavasi, A. Fiorio Pla, L. Munaron, C. Morterra, *Acta Biomater.* **2009**, 5, 1211.
- [124] L. Courthéoux, J. Lao, J.-M. Nedelec, E. Jallot, *J. Phys. Chem. C* **2008**, 112, 13663.
- [125] A. M. El-Kady, A. F. Ali, *Ceram. Int.* **2012**, 38, 1195.
- [126] M. Jarosz, M. Olbert, G. Wyszogrodzka, K. Młyniec, T. Librowski, *Inflammopharmacology* **2017**, 25, 11.
- [127] M. Sohrabi, B. E. Yekta, H. Rezaie, M. R. Naimi-Jamal, A. Kumar, A. Cochis, M. Miola, L. Rimondini, *Ceram. Int.* **2021**, 47, 12526.
- [128] M. D. O'Donnell, R. G. Hill, *Acta Biomater.* **2010**, 6, 2382.
- [129] V. Nicolini, G. Malavasi, L. Menabue, G. Lusvardi, F. Benedetti, S. Valeri, P. Luches, *J. Mater. Sci.* **2017**, 52, 8845.
- [130] A. A. El-Khesheh, F. A. Khaliifa, E. A. Saad, R. L. Elwan, *Ceram. Int.* **2008**, 34, 1667.

- [131] A. K. Chatterjee, R. Chakraborty, T. Basu, *Nanotechnology* **2014**, 25, 135101.
- [132] S. M. Salman, S. N. Salama, H. A. Abo-Mosallam, *Ceram. Int.* **2012**, 38, 55.
- [133] T. Kasuga, M. Yoshida, A. J. Ikushima, M. Tuchiya, H. Kusakari, *J. Am. Ceram. Soc.* **1992**, 75, 1884.
- [134] J. Wu, S. Wang, Z. Zheng, J. Li, *Regen. Ther.* **2022**, 21, 122.
- [135] W. Zheng, Z. Bai, S. Huang, K. Jiang, L. Liu, *Int. J. Mol. Sci.* **2022**, 23, 12670.
- [136] M. S. Fernandes, E. C. Kukulka, J. R. de Souza, A. L. S. Borges, T. M. B. Campos, G. P. Thim, L. M. R. de Vasconcelos, *J. Polym. Res.* **2022**, 29, 370.



**Farnaz Ghorbani** is an Alexander von Humboldt postdoctoral research fellow at the Friedrich-Alexander University (FAU) Erlangen-Nuremberg (Germany) and visiting researcher at University College London (London, UK). Formerly, Ghorbani held a postdoctoral position at the Orthopedic Surgery Department of Fudan University Pudong Medical Center (Shanghai, China). Also, she has been awarded the Marie Skłodowska-Curie Career-FIT PLUS Research Fellowship and a Bavarian Funding Programme for the Initiation of International Projects. She employs biomaterials for tissue engineering applications, and in particular, her current research focuses on osteochondral defect repair using hierarchical structures.



**Liliana Liverani** is currently R&D officer at DGS S.p.A. (Italy) and visiting researcher at the Institute of Biomaterials, Friedrich-Alexander University (FAU) Erlangen-Nuremberg (Germany). At the same Institute she has been a senior researcher for almost 7 years. She joined FAU in 2015, when she was awarded a Marie Skłodowska Curie Individual Fellowship. From 2017 to 2021, she was the coordinator for the training of visiting researchers at FAU for 2 EU projects. From 2019 to 2021, she served in the Young Scientists Forum of the European Society for Biomaterials as National Chapters Liaison Officer. Her main research interests are in the field of materials synthesis, processing and characterization, application of AI, mainly focused on healthcare applications. She is the author/co-author of 60+ scientific papers, and she is also involved in educational activities.



**Aldo R. Boccaccini** is Professor of Biomaterials and Head of the Institute of Biomaterials at Friedrich-Alexander University Erlangen-Nuremberg, Germany. He is a visiting professor at Imperial College London, UK. Boccaccini graduated from Instituto Balseiro, Argentina (1987) and earned the Doctorate in Engineering from RWTH Aachen University, Germany (1994). He held post-doctoral appointments at University of Birmingham (UK) and University of California, San Diego (USA). He received an honorary doctorate from Abo Akademi University (Finland) in 2022. The research activities of Prof. Boccaccini are in the field of ceramics, glasses, and composites for biomedical, functional, and/or structural applications with focus on bioactive scaffolds for tissue engineering.



**Judith A. Roether** studied Materials Science as well as Environmental Engineering in London, UK, where she also completed her Ph.D. on bioactive bone cements for orthopaedic applications at Guy's Hospital (King's College London) in 2005. She was then post-doctoral researcher at Imperial College London working on a European project. In 2009, she moved to Friedrich-Alexander University (FAU) Erlangen-Nuremberg, Germany, where she is still based today; working at the Institute for Polymer Materials, Department of Materials Science and Engineering. Her research areas include electrospinning, bioactive glasses, and biocomposite materials.